NASA MEMO 2-23-59E

NASA

MEMORANDUM

A NUMERICAL METHOD FOR OBTAINING MONOENERGETIC NEUTRON FLUX DISTRIBUTIONS AND TRANSMISSIONS IN MULTIPLE-REGION SLABS

By Harold Schneider

Lewis Research Center
Cleveland, Ohio

NATIONAL AERONAUTICS AND SPACE ADMINISTRATION
WASHINGTON
February 1959

NATIONAL AERONAUTICS AND SPACE ADMINISTRATION

MEMORANDUM 2-23-59E

A NUMERICAL METHOD FOR OBTAINING MONOENERGETIC NEUTRON FLUX DISTRIBUTIONS AND TRANSMISSIONS IN MULTIPLE-REGION SLABS

By Harold Schneider

SUMMARY

This method is investigated for semi-infinite multiple-slab configurations of arbitrary width, composition, and source distribution. Isotropic scattering in the laboratory system is assumed.

Isotropic scattering implies that the fraction of neutrons scattered in the i^{th} volume element or subregion that will make their next collision in the j^{th} volume element or subregion is the same for all collisions. These so-called "transfer probabilities" between subregions are calculated and used to obtain successive-collision densities from which the flux and transmission probabilities directly follow.

For a thick slab with little or no absorption, a successive-collisions technique proves impractical because an unreasonably large number of collisions must be followed in order to obtain the flux. Here the appropriate integral equation is converted into a set of linear simultaneous algebraic equations that are solved for the average total flux in each subregion.

When ordinary diffusion theory applies with satisfactory precision in a portion of the multiple-slab configuration, the problem is solved by ordinary diffusion theory, but the flux is plotted only in the region of validity. The angular distribution of neutrons entering the remaining portion is determined from the known diffusion flux and the remaining region is solved by higher order theory.

Several procedures for applying the numerical method are presented and discussed. To illustrate the calculational procedure, a symmetrical slab in vacuum is worked by the numerical, Monte Carlo, and P_3 spherical harmonics methods. In addition, an unsymmetrical double-slab problem is solved by the numerical and Monte Carlo methods. The numerical approach proved faster and more accurate in these examples. Adaptation of the method to anisotropic scattering in slabs is indicated, although no example is included in this paper.

INTRODUCTION

In order to solve a multiple-slab configuration of arbitrary width, composition, and source distribution for the monoenergetic neutron flux distribution and the number of transmissions, recourse to a number of powerful methods is available. Wherever diffusion theory does not apply, the spherical harmonics (ref. 1), Monte Carlo (ref. 2), and S_n (ref. 3) methods can be used.

The present discussion concerns a numerical method that accurately approximates the exact solution to many slab problems with a reasonable amount of calculation. Isotropic scattering of monoenergetic neutrons in the laboratory system is assumed. The numerical method is essentially a procedure for solving the integral equation for the total flux given in reference 1 (p. 78).

The numerical method was worked out in principle by DeMarcus and Nelson (ref. 4) and was obtained by the author as a natural consequence of working slab problems by Monte Carlo. This method is relatively easy to apply when at least some absorption is present and/or for thin slabs where an appreciable leakage occurs - in other words, where too many collisions need not be followed in order to obtain the flux; these are the conditions under which diffusion theory is generally inadequate. For the other extreme, a thick slab with little or no absorption, a set of simultaneous algebraic equations can be solved for the average total flux in each subregion. When the diffusion-theory solution is known to apply with satisfactory precision in a portion of the slab array, this information can be utilized to great advantage in simplifying the numerical calculation. Also, it proves feasible in a number of cases to treat a multiple-slab configuration as essentially a single-slab problem with the resulting simplification.

For purposes of illustration, a simple slab containing a centrally located isotropic source plane and surrounded by vacuum was chosen. A scattering probability of 8/10 per collision and a slab half-width of 0.781 mean free paths were also chosen.

The integrals for the probabilities of transmission with no collision and one collision were analytically formulated and evaluated. The numerical-method flux and the number of neutrons transmitted with exactly K collisions, K = 0,1,2, . . . 19, were obtained and compared with a Monte Carlo calculation. The numerical-method flux was also compared with the P_3 spherical harmonics and P_1 diffusion-theory fluxes.

Values of the slab half-width were successively changed to 1/5 and 5 total mean free paths, and the numerical-method flux was obtained and compared with diffusion theory for these cases.

As a second example, a configuration in vacuum consisting of two contiguous slabs of different absorption and scattering properties was solved. An isotropic source plane was assumed at the left extreme boundary. Distributed volume sources were avoided to facilitate the Monte Carlo calculation. Twenty-eight collisions were followed in the Monte Carlo and numerical successive-collisions treatment. The total flux and the number of transmissions after exactly K collisions were recorded and compared. The total flux was also obtained numerically by solving the appropriate set of simultaneous algebraic equations discussed in the text.

SYMBOLS

A,B,C, . . .	regions or slabs A,B,C, . . .
$A_\nu, B_\nu; \nu=1,2,3,4$	arbitrary constants
a,b,c, . . .	widths in centimeters of slabs I, II, III, . . . or slabs A,B,C, . . .
$a_0, a_1, \ldots b_0, b_1$	nuclear constants of region A and B (defined in appendix F)
$F, F(x,\mu)$	transport flux
$F_l(x)$	coefficient of the l^{th} Legendre polynomial of μ in series expansion of transport flux
$G; G_{q_1,0}, G_{0,q_2}$	matrices defined by equations (3) and (12)
g	number of spherical zones of width $d\mu$ representing equal areas on a hemisphere of unit radius
$H; H_{1,0}; H_{0,2}; H_{1,2}$	matrices defined by equations (3), (12), and (13)
I	q-by-q- unit matrix
i=1,2,3, . . .	index denoting specific subregion (subslab) of given slab (subregions are numbered consecutively from left to right)
j=1,2,3, . . .	index denoting specific subregion (subslab) of given slab
K	number of collisions a neutron has suffered

ΔL	subregion width in total mean free paths
L'	distance in mean free paths from point lying anywhere in subregion i to center of subregion j; neutron is assumed to scatter in i and then collide in j
L_r	distance in mean free paths from center of subregion i to center of subregion j, where $r = \|j-i\| = 1,2 \ldots$
l, l'	distances in mean free path units defined in connection with equation (A3) and sketch (c), page 26
l_r	distance in mean free paths from boundary of one subregion to center of another or conversely
N^s, N_K^s	matrices defined by equations (5) and (3)
$n_K^s(i)$	number of neutrons scattered per second from K^{th} collision in subregion i; in particular, $n_0^s(i)$ represents primary volume source in i
$n(x_0,\mu)d\mu$	number of neutrons per square centimeter per second arriving at x_0 and having direction cosines in $d\mu$ about μ
$n^s(i)$	total number of neutrons per second scattered in i for all collisions
n^T	total number of neutrons transmitted after one or more collisions
n_K^T	number of neutrons transmitted in exactly K collisions
P	matrix defined by equation (15)
$P(\Delta L_I, \Delta L_{II})$	transfer probability between unequal subregions as measured in units of mean free path
$P(x',x)dx$	kernel of equation (10), given by equation (A2)
$P_{i,j}$ or $P(X_i', X_j)\Delta X_j$	probability that a neutron will make its next collision in subregion j after being isotropically scattered in subregion i
$P_l(\mu)$	l^{th} Legendre polynomial

P_r or $P(L_r,\Delta L)$	transfer probability between subregions of equal width, as measured in units of total mean free path (eq. (A8a)
P_0	probability that next collision will occur in subregion in which neutron scattered
P_1^{LR}	probability that a neutron will make its first collision to left of source plane and be transmitted through right-hand boundary without a second collision
$P^T(l)$ or $P^T(x',x)$	probability that a neutron scattered or born isotropically at x' will be transmitted through a boundary l mean free paths away with no intervening collisions
P_K^{-T}, P_K^T	probability of a source neutron being transmitted through extreme left or right boundaries, respectively, in exactly K collisions
$p(\mu',\mu)d\mu$	given a neutron having direction cosine μ' and undergoing scattering collision that may or may not be isotropic; this expression represents probability of finding neutron velocity in direction $d\mu$ about μ after collision
p_r; r=1,2, . . .	transfer probability from source plane at boundary of a subregion to within r^{th} adjacent subregion
q	total number of subregions in given configuration
R	random number
r	integer 1,2,3, . . . equaling j-i
S	source
$S(L')dL'$	source in infinitesimal strip of width dL'
ΔX	subregion width in centimeters
X_i, X_j	x coordinates of centers of i^{th} and j^{th} subregions
x_0, x_L, x_R	x coordinates of interface and extreme left and right boundaries, respectively
$\beta_\nu, \gamma_\nu, \delta_\nu, \lambda_\nu, \varkappa_1, \varkappa_2$	defined by equation (F3)

$\delta(x)$	Dirac delta function
δ_h	probability that a neutron with direction cosine μ_h will pass through a single subregion without collision
$\delta_{h,l}$	Kronecker delta = $\begin{cases} 0, h \neq l \\ 1, h = l \end{cases}$
ϵ	error per collision resulting from assumption that all scattering collisions within a subregion take place at center
$\lambda, (\lambda/\lambda_s)$	total mean free path and scattering probability per collision
μ	equals cosine of ξ
ξ	angle between $\vec{\Omega}$ and the x axis
ρ	radial distance to next collision point
Σ	equals $1/\lambda$
Φ	1-by-q matrix for flux in each subregion
$\varphi(i)$	average total flux in subregion i
$\vec{\Omega}$	unit vector in direction of neutron velocity
$d\vec{\Omega}$	element of solid angle about $\vec{\Omega}$

Subscripts and superscripts:

h	specific solid angle in direction space
L	left extreme boundary
R	right extreme boundary
s	scattering
T	transmitted
I, II	specific slab, medium, or region

ANALYSIS

The assumption of isotropic scattering in the laboratory system is a good approximation for neutron collisions with heavy nuclei. Isotropic scattering implies that the direction of neutron travel after collision

is unrelated to the direction of travel before collision. Thus, the probability $P_{i,j}$ that neutrons scattering in volume element i will make their next collision in volume element j is the same for all collisions. For a one-dimensional or semi-infinite slab, i and j refer to subslabs or subregions that hereafter will be taken to be equal in width in a given slab. This implies that $P_{i,j} = P_{j,i}$. Furthermore, if these subregions are numbered consecutively, $P_{i,j} = P_{i+1,j+1}$. This means, for example, that $P_{1,3} = P_{3,5} = P_{6,4} = P_{8,6}$, and so forth. The transfer probability, henceforth called P_r, therefore depends on a single index r and is characteristic of slab geometry. Thus, given that a neutron is scattered in any subregion, P_0 is the probability that it will make its next collision in the same subregion, P_1 in the adjacent subregion, P_2 in the second adjacent subregion, and so forth. The P_r's do not vary from collision to collision and can therefore be calculated once and used to obtain the $(K+1)^{st}$ collision density distribution from the K^{th}. For a slab with q equal subregions, there are q different transfer probabilities.

For problems involving spherical symmetry, the sphere would be divided into q spherical shells of equal width. Here, however, the transfer probability $P_{i,j}$ from shell i to shell j is not equal to that from j to i, $P_{j,i}$. Also, $P_{i,i} \neq P_{j,j}$. Thus, there are q^2 different transfer probabilities as opposed to the q probabilities of the slab case.

In cylindrical geometry there would also be q^2 $P_{i,j}$'s between concentric cylindrical shells. This paper considers only the slab case.

Single-Slab Analysis

Consider a typical slab of width "a" centimeters divided into q subregions of equal width, numbered from left to right by the index i.

Let λ and λ_s be the total and scattering mean free paths of the given medium and let the width of each subregion be ΔL total mean free paths. Furthermore, define $n_K^s(i)$ to be the number of neutrons scattered per second from the K^{th} collision in subregion i. Then $n_0^s(i)$, for example, represents the given initial volume source in i, and $n_1^s(i)$ represents the number of first-collision scatterings in i. If ΔL has been chosen sufficiently small,

$$\Delta L = \frac{\Delta X}{\lambda} = \frac{a}{q\lambda}$$

then the sources within each subregion can be lumped at its center with negligible error (appendix A). The transfer probability is then computed from the center of the i^{th} subregion to within the $i+r^{th}$ subregion, after which the transferred neutrons are in turn lumped at the center of the latter subregion.

The transfer probability P_r is a function only of the distance L_r between the centers of the two subregions involved and of the subregion width ΔL, all in units of total mean free path. Although $L_r = r\Delta L$, $r = 1,2, \ldots, (q-1)$, P_r is denoted by $P(L_r,\Delta L)$ as formulated and evaluated in appendix A.

Initial and subsequent collision densities arising from distributed isotropic volume sources. - The specified volume sources are assumed to be lumped into isotropic source planes located at the centers of the subregions. After $P_0, P_1, \ldots, P_{q-1}$ are calculated from equations (A8a) and (A9), the number of $(K+1)^{st}$ collision scattering hits in subregion i may be obtained by summing the contributions to i from the previous or K^{th} collision in all of the subregions. Mathematically stated,

$$n^s_{K+1}(i) = \frac{\lambda}{\lambda_s}\left[\sum_{\alpha=1}^{i-1} n^s_K(i-\alpha)P_\alpha + \sum_{\alpha=i}^{q} n^s_K(\alpha)P_{\alpha-i}\right] \qquad i = 1,2, \ldots, q \quad (1)$$

where the first summation represents the input into i from subregions to the left of i and the second summation represents the input from subregions to the right of i, including i itself. The quantity λ/λ_s gives the fraction of the $(K+1)^{st}$ collision hits that scatter. Setting $K = 0$ in equation (1) gives the first-collision distribution due to the distributed primary volume sources $n^s_0(i)$. Successive-collision distributions are obtained by successively increasing K by 1 unit and evaluating $n^s_{K+1}(i)$ from equation (1). The total number of scattering hits for all collisions is given by

$$n^s(i) = \sum_{K=1}^{\infty} n^s_K(i) \qquad (2)$$

A sufficient number of collisions are followed until $n^s(i)$ does not change appreciably.

First-collision distribution due to isotropic source plane at interface between subregions. - If the source plane is located at an interface between subregions, another set of transfer probabilities p_r can be calculated from equation (A8) as before, but with

$$L' = \left(r - \frac{1}{2}\right)\Delta L \qquad r = 1,2, \ldots \tag{A8b}$$

instead of

$$L' = r\,\Delta L \qquad r = 1,2, \ldots \tag{A8a}$$

Thus, p_1 represents the fraction of the source-plane neutrons that will collide in the first adjacent subregion, p_2 in the second adjacent subregion, p_3 in the third, and so forth. Once the initial-collision distribution has been determined, successive-collision distributions follow from equation (1).

If a reasonable amount of absorption is present and/or the slab is sufficiently thin so that a large number of collisions are not required in order for the number of scattering hits to converge, then equation (2) may be utilized for machine calculation. For cases where convergence is slow, a collision-by-collision technique is impractical, so a matrix treatment, suggested in reference 4, is used.

Matrix formulation of equation (1). - Define matrices H, G, and N_K^s as

$$H \equiv \frac{\lambda}{\lambda_s}\,G \equiv \frac{\lambda}{\lambda_s}\begin{bmatrix} P_0 & P_1 & P_2 & -- & -- & -- & -- & P_{q-1} \\ P_1 & P_0 & P_1 & P_2 & -- & -- & -- & \text{----} \\ P_2 & P_1 & P_0 & P_1 & P_2 & -- & -- & \text{----} \\ -- & P_2 & P_1 & P_0 & P_1 & P_2 & -- & \text{----} \\ -- & -- & P_2 & P_1 & P_0 & P_1 & P_2 & \text{----} \\ -- & -- & -- & P_2 & P_1 & P_0 & P_1 & P_2 \\ -- & -- & -- & -- & P_2 & P_1 & P_0 & P_1 \\ P_{q-1} & -- & -- & -- & -- & P_2 & P_1 & P_0 \end{bmatrix} \tag{3}$$

$$N_K^s \equiv \left[n_K^s(1),\ n_K^s(2),\ \ldots,\ n_K^s(q)\right]$$

$$K = 0,1,2, \ldots$$

Equation (1) can then be written in matrix form as

$$N^S_{K+1} = N^S_K H \qquad K = 0,1,2, \ldots \tag{4}$$

The symbol N^S_0 defines the 1-by-q matrix for the given original volume sources. The matrix to be found is N^S, a 1-by-q matrix whose elements $n^S(i)$ represent the total number of scattering hits in subregion i for all collisions (eq. (2)).

$$\text{Matrix } N^S \equiv [n^S(1), n^S(2), \ldots, n^S(q)]$$

From equation (4) it follows that

$$N^S_{K+1} = N^S_0 H^{K+1}$$

or

$$N^S = \sum_{K=0}^{\infty} N^S_0 H^{K+1} = \frac{N^S_0 H}{I-H}$$

where I is a q-by-q - unit matrix. Therefore,

$$N^S(I-H) = N^S_0 H \tag{5}$$

The quantities H, I-H, and N^S_0 are known matrices given by equation (3). Hence, equation (5) represents q linear simultaneous algebraic equations for the unknown $n^S(i)$. If $n^S(i)$ has been found, the average total flux in each subregion is computed as

$$\Phi(i) = n^S(i) \frac{\lambda_S}{\Delta X} \qquad i = 1,2, \ldots, q \tag{6}$$

where ΔX is the width of subregion i in centimeters. In some cases it will be more economical to utilize equation (5) to obtain the converged flux, while in others a collision-by-collision technique as implied by equation (4) will be preferable.

Integral equation for total flux. - It will now be shown that equation (5) corresponds to numerically solving an integral equation for the total flux.

Denote the x coordinate of the center of the i^{th} subregion in which the neutron scatters by X'_i. Let X_j be the x coordinate of the center of the j^{th} subregion to which the neutrons are transferred for their next collision. Replace the transfer probabilities in equation (1)

by their equivalent $P(X_i',X_j)\Delta X_j$ and replace $n^s_{K+1}(i)$ by $n^s_{K+1}(X_j)\Delta X_j$. Summing both sides of equation (1) over-all collisions gives

$$\sum_{K=0}^{\infty} n^s_{K+1}(X_j)\Delta X_j = \frac{\lambda}{\lambda_s}\left[\sum_{i=1}^{q} n^s_0(X_i')\Delta X_i' \; P(X_i',X_j)\Delta X_j + \sum_{i=1}^{q}\sum_{K=1}^{\infty} n^s_K(X_i')\Delta X_i' \; P(X_i',X_j)\Delta X_j\right] \quad (7)$$

Equation (7) states that the total scattering rate for all collisions in ΔX_j is the number of first-collision scatterings plus the number of subsequent scatterings as represented by the last term. From equations (2) and (6), there follows, after dividing through by $\Delta X_j = \Delta X_i'$,

$$\Phi(X_j) = \lambda \sum_{i=1}^{q} n^s_0(X_i')\Delta X_i' \; P(X_i',X_j) + \frac{\lambda}{\lambda_s}\sum_{i=1}^{q} \Phi(X_i')\Delta X_i' \; P(X_i',X_j) \quad (8)$$

With the subscript i and/or j affixed to n^s_0, P, and Φ, equation (8) becomes

$$\Phi_j = \lambda \sum_{i=1}^{q} n^s_{0,i}P_{i,j} + \frac{\lambda}{\lambda_s}\sum_{i=1}^{q} \Phi_i P_{i,j} \qquad j = 1,2, \ldots, q \quad (9)$$

Equation (9) represents q linear simultaneous algebraic equations. In matrix form, it is identically equation (5) with N^s replaced by $\frac{1}{\lambda_s}\Phi$.

Allowing $\Delta X_i' \to 0$ in equation (8) gives the Fredholm-type integral equation for the total flux (ref. 1):

$$\Phi(x) = \lambda \int_{x'} n^s_0(x') \; P(x',x)dx' + \frac{\lambda}{\lambda_s}\int_{x'} \Phi(x') \; P(x',x)dx' \quad (10)$$

The kernel $P(x',x)$ is given by equation (A2). The successive-collisions technique of equation (4) therefore corresponds to solving equation (10).

Multiple-Slab Analysis

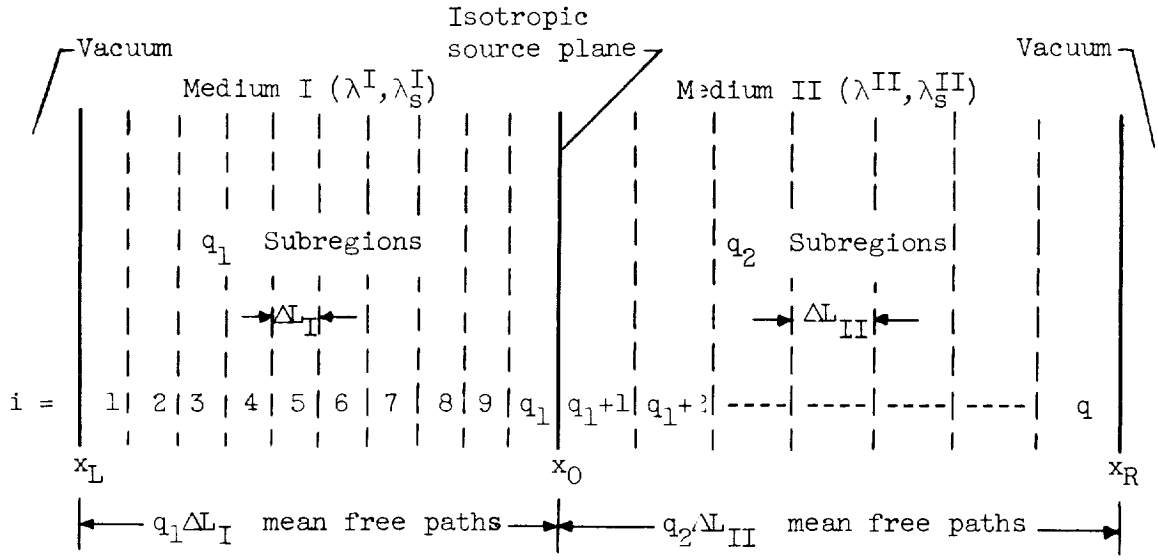

Sketch (a). - Multiple-slab configuration.

Angular distribution of neutrons. - Sketch (a) displays two contiguous slabs. Additional slabs need not be considered because all the numerical techniques required are illustrated by this double-slab problem. An isotropic source plane is assumed at the interface x_0.

The neutron flux is obtained in the first slab by following neutrons from collision to collision within this slab by means of equation (4) or by solving the q_1 simultaneous algebraic equations represented by equation (5). The second slab is entered by means of an angular distribution $n(x_0,\mu)d\mu$ that is determined from the known flux. The angular distribution is derived as equation (B2) and represents the number of neutrons per square centimeter per second arriving at x_0 and having direction cosines lying in $d\mu$ about μ.

The isotropic source plane and $n(x_0,\mu)d\mu$ determine the first-collision distribution in the second slab. Neutrons are followed therein until its flux converges. A new angular distribution is computed for reentry into the first slab. These neutrons are followed, giving an augmented flux that represents the combined effect of the original neutrons plus those backscattered once from the second slab. The latter slab is entered a second time, and so forth. Thus, neutrons are followed in one slab at a time, with the other being entered by means of the angular distribution. This procedure is not feasible when an excessive

number of interface crossings is required to achieve a converged flux everywhere. This difficulty does not arise if either slab is a reasonable absorber.

The angular distribution represents an anisotropic source plane at the interface. The first-collision distribution of these neutrons is computed by dividing the angular hemispherical region - to the right of the interface, for example - into a grid of g solid angles. The proper number of neutrons is sent into each solid angle by means of $n(x_0,\mu)d\mu$. The exponential attenuation law gives the fraction colliding in each subregion of the second slab for direction cosine μ. Summing over all solid angles yields the first-collision distribution as expressed by equation (B5). Once this is known, subsequent collision distributions follow from equation (4), or the final distribution follows from equation (5) with N_1^s in the right-hand term.

Numerical treatment of anisotropic scattering in slabs. - Anisotropic scattering in slabs can be treated in an analogous manner by:

(1) Assuming the anisotropic volume sources for the next collision to be lumped into a source plane at the center of a subregion.

(2) Utilizing an expression $p(\mu',\mu)d\mu$ which gives the probability that a neutron having direction cosine μ' will be found in $d\mu$ about μ after undergoing a scattering collision.

(3) Applying the technique of equations (B5) and (B6) to each source plane to determine the number of neutrons that will make their next collision in each of the subregions for a given μ.

(4) Repeating steps (1), (2), and (3) for the other μ's and proceeding to the next collision. The procedure is an order of magnitude more involved here because the angular distribution must be recorded at the center of each subregion in following successive collisions, whereas it was unnecessary to do this for the isotropic case.

Reduction of multiple-slab to single-slab configuration. - When the number of interface crossings required becomes excessive, the angular-distribution approach becomes impractical. Noting that the transfer probabilities (eq. (A8)) in a given slab are functions only of the subregion width ΔL, one attempts to choose $\Delta L_I = \Delta L_{II}$. The transfer probabilities of both slabs become identical, and a single set of transfer probabilities applies throughout. A two-slab problem has then been reduced to a single-slab problem with the resulting simplification:

The relation $\Delta L_I = \Delta L_{II}$ implies that

$$\frac{a}{q_1\lambda^I} = \frac{b}{q_2\lambda^{II}}$$

or

$$q_2 = \left(\frac{\lambda^I}{\lambda^{II}} \frac{b}{a}\right) q_1 \qquad q_1, q_2 = 1,2,3, \ldots \tag{11}$$

where a and b are the respective widths in centimeters of slabs I and II, λ the total mean free path, and q_1 the number of subregions in slab I.

Equation (11) can be rigorously satisfied only when the given numerical quantity in parentheses is an integer. Otherwise, a set of values should be sought for q_1 and q_2 satisfying (11) such that:

(1) Rounding off to the nearest integers alters the given physical dimensions of the configuration a negligible amount.

(2) The values of q_1 and q_2 are not excessively large for calculation purposes.

(3) The values of q_1 and q_2 are sufficiently large that the subregions have negligible lumping error.

When these three criteria can be met, it is perhaps best to choose the number of subregions in each slab according to equation (11). Thus, a multiple-slab problem can be worked as a single slab. However, the colliding neutrons must be weighted by the scattering probability λ/λ_s of the medium in which they collide. Equation (1) must then be modified to read:

$$n^s_{K+1}(i) = \left(\frac{\lambda}{\lambda_s}\right)^I \left[\sum_{\alpha=1}^{i=1} n^s_K(i-\alpha) P_\alpha + \sum_{\alpha=i}^{q} n^s_K(\alpha) P_{\alpha-i}\right] \qquad i = 1,2, \ldots, q_1$$

$$n^s_{K+1}(i) = \left(\frac{\lambda}{\lambda_s}\right)^{II} \left[\sum_{\alpha=1}^{i-1} n^s_K(i-\alpha) P_\alpha + \sum_{\alpha=i}^{q} n^s_K(\alpha) P_{\alpha-i}\right] \qquad \begin{matrix} i = q_1+1, q_1+2, \ldots, q \\ q = q_1 + q_2 \end{matrix}$$

Define matrix $G_{q_1,0}$ to be identical to matrix G of equation (3) in the first q_1 columns with zero elements in the remaining columns. Also define G_{0,q_2} to be identical to G in the last q_2 columns with zero elements in the others. Defining matrices $H_{1,0}$ and $H_{0,2}$ as

$$\left.\begin{aligned} H_{1,0} &\equiv \left(\frac{\lambda}{\lambda_s}\right)^{I} G_{q_1,0} \\ H_{0,2} &\equiv \left(\frac{\lambda}{\lambda_s}\right)^{II} G_{0,q_2} \end{aligned}\right\} \tag{12}$$

equation (4) becomes

$$\left.\begin{aligned} N^S_{K+1} &= N^S_K(H_{1,0} + H_{0,2}) \equiv N^S_K H_{1,2} \\ N^S_K &\equiv \left[n^S_K(1),\ n^S_K(2),\ \ldots,\ n^S_K(q)\right] \end{aligned}\right\} \quad K = 0,1,2,\ \ldots \tag{13}$$

Following the same procedure used in deriving equation (5) gives

$$N^S(I - H_{1,2}) = N^S_0 H_{1,2} \tag{14}$$

Equation (13) is utilized in a collision-by-collision procedure, whereas equation (14) gives $n^S(i)$ directly when the q simultaneous algebraic equations represented by (14) are solved.

Transfer probabilities between unequal subregions lying in different media. - When it is impractical to use the angular distribution to pass from one slab into the other or to make the ΔL's equal, transfer probabilities between unequal subregions lying in different media can be used. These transfer probabilities eliminate the need for the angular distribution but require many more computer storage locations. They are calculated from equation (A11).

Referring to sketch (a), $P^{(1)}_{i,j}$ is defined as the transfer probability between subregions i and j lying exclusively in medium I and $P^{(2)}_{i,j}$ as the transfer probability for i and j lying exclusively in medium II. If i lies in medium I and j in medium II or conversely, then the transfer probability is written as $P_{i,j}$ and $P_{j,i}$, respectively.

A matrix P is defined as

$$P \equiv \left[\begin{array}{c|c} \left(\frac{\lambda}{\lambda_s}\right)^{I} P^{(1)}_{i,j} & \left(\frac{\lambda}{\lambda_s}\right)^{II} P_{i,j} \\ q_1\text{-by-}q_1 \text{ matrix} & q_1\text{-by-}q_2 \text{ matrix} \\ \hline \left(\frac{\lambda}{\lambda_s}\right)^{I} P_{j,i} & \left(\frac{\lambda}{\lambda_s}\right)^{II} P^{(2)}_{i,j} \\ q_2\text{-by-}q_1 \text{ matrix} & q_2\text{-by-}q_2 \text{ matrix} \end{array}\right] \equiv \left[\begin{array}{c|c} A & B \\ \hline C & D \end{array}\right] \tag{15}$$

Since $P^{(1)}_{i,j}$ and $P^{(2)}_{i,j}$ are the usual transfer probabilities between subregions lying in the same medium, they can be denoted by $P^{(1)}_{r}$ and $P^{(2)}_{r}$, respectively, to be consistent with the previous notation. If there are $q_1 = 6$ subregions in medium I, for example, and $q_2 = 4$ subregions in medium II ($q = q_1 + q_2 = 10$), then equation (15) reads

$$A = \left(\frac{\lambda}{\lambda_s}\right)^{I} \begin{bmatrix} P^{(1)}_0 & P^{(1)}_1 & P^{(1)}_2 & P^{(1)}_3 & P^{(1)}_4 & P^{(1)}_5 \\ P^{(1)}_1 & P^{(1)}_0 & P^{(1)}_1 & P^{(1)}_2 & P^{(1)}_3 & P^{(1)}_4 \\ P^{(1)}_2 & P^{(1)}_1 & P^{(1)}_0 & P^{(1)}_1 & P^{(1)}_2 & P^{(1)}_3 \\ P^{(1)}_3 & P^{(1)}_2 & P^{(1)}_1 & P^{(1)}_0 & P^{(1)}_1 & P^{(1)}_2 \\ P^{(1)}_4 & P^{(1)}_3 & P^{(1)}_2 & P^{(1)}_1 & P^{(1)}_0 & P^{(1)}_1 \\ P^{(1)}_5 & P^{(1)}_4 & P^{(1)}_3 & P^{(1)}_2 & P^{(1)}_1 & P^{(1)}_0 \end{bmatrix} \qquad B = \left(\frac{\lambda}{\lambda_s}\right)^{II} \begin{bmatrix} P_{1,7} & P_{1,8} & P_{1,9} & P_{1,10} \\ P_{2,7} & P_{2,8} & P_{2,9} & P_{2,10} \\ P_{3,7} & P_{3,8} & P_{3,9} & P_{3,10} \\ P_{4,7} & P_{4,8} & P_{4,9} & P_{4,10} \\ P_{5,7} & P_{5,8} & P_{5,9} & P_{5,10} \\ P_{6,7} & P_{6,8} & P_{6,9} & P_{6,10} \end{bmatrix}$$

$$C = \left(\frac{\lambda}{\lambda_s}\right)^{I} \begin{bmatrix} P_{7,1} & P_{7,2} & P_{7,3} & P_{7,4} & P_{7,5} & P_{7,6} \\ P_{8,1} & P_{8,2} & P_{8,3} & P_{8,4} & P_{8,5} & P_{8,6} \\ P_{9,1} & P_{9,2} & P_{9,3} & P_{9,4} & P_{9,5} & P_{9,6} \\ P_{10,1} & P_{10,2} & P_{10,3} & P_{10,4} & P_{10,5} & P_{10,6} \end{bmatrix} \qquad D = \left(\frac{\lambda}{\lambda_s}\right)^{II} \begin{bmatrix} P^{(2)}_0 & P^{(2)}_1 & P^{(2)}_2 & P^{(2)}_3 \\ P^{(2)}_1 & P^{(2)}_0 & P^{(2)}_1 & P^{(2)}_2 \\ P^{(2)}_2 & P^{(2)}_1 & P^{(2)}_0 & P^{(2)}_1 \\ P^{(2)}_3 & P^{(2)}_2 & P^{(2)}_1 & P^{(2)}_0 \end{bmatrix}$$

where the double-subscript elements are the transfer probabilities between unequal subregions. None of the elements in the B and C matrices are equal.

With matrices N^s_K and N^s defined as before,

$$N^s_{K+1} = N^s_K P \tag{16}$$

$$N^s(I - P) = N^s_0 P \tag{17}$$

Matrix I is a q-by-q-unit matrix. Equation (16) is used to follow neutrons from collision to collision in the configuration when $\Delta L_I \neq \Delta L_{II}$. When convergence of (16) is slow, equation (17), which represents q simultaneous algebraic equations for the total number of scattering hits in each subregion, is used.

Combined application of diffusion theory and numerical method. - Assume, for example, a thick slab having an isotropic source plane at the

left extreme boundary and located in vacuum. Ordinary diffusion theory applies accurately in the region of about three or more mean free paths from the source. Denote this as region II. The entire slab is solved by ordinary diffusion theory. The resulting flux, however, is plotted only in region II because an exact transport-theory calculation would yield substantially the same curve only in this region. This leaves the region from the source plane up to three mean free paths to be worked by higher order theory.

The flux in region II includes neutrons that have crossed and re-crossed the interface any number of times. The angular distribution into region I arises from this flux and is calculated by equation (B3). It therefore represents the final angular distribution and is consequently calculated only once. Thereafter, region II is treated as a vacuum in following the neutrons in region I.

The first-collision distribution in region I, due to the angular distribution at the interface, is obtained by equation (B6). To this is added the contribution from the original source plane at the left boundary. By knowing the first-collision distribution, successive-collision densities are calculated in the usual manner, utilizing the transfer probabilities of region I. The resultant numerical flux completes the distribution for the entire slab.

Calculation of various quantities of interest in a slab calculation. - From the total number of scattering hits $n^s(i)$ in each subregion of the given slab, the average total flux is computed by equation (6).

The total absorption rate in each subregion and consequently in the entire slab is computed by

$$\frac{\lambda_s}{\lambda_{capt}} \sum_{i=1}^{q} n^s(i) \tag{18}$$

Since the number of neutrons per second entering the given slab - that is, the production - is known, then

$$\text{Total leakage} = \text{Production} - \text{Absorption}$$

where the absorption term is given by expression (18).

The total number of neutrons n^T transmitted outward through the extreme left or right boundaries from one or more collisions within the slab is

$$\left.\begin{aligned} \sum_{i=1}^{q} n^S(i)P^T(l_i) &= n_L^T \\ \sum_{i=1}^{q} n^S(i)P^T(l_{q+1-i}) &= n_R^T \end{aligned}\right\} \qquad (19)$$

where $l_r = \left(r - \frac{1}{2}\right)\Delta L$ and $P^T(l)$ is defined by equation (A6).

The angular distribution of these neutrons is (appendix B):

$$\left.\begin{aligned} n(x_L, |\mu_h|)d\mu &= \sum_{i=1}^{q} n^S(i)e^{-l_i/|\mu_h|}\,\frac{1}{2}\,d\mu \qquad \mu_h < 0 \\ n(x_R, |\mu_h|)d\mu &= \sum_{i=1}^{q} n^S(i)e^{-l_{q+1-i}/|\mu_h|}\,\frac{1}{2}\,d\mu \qquad \mu_h > 0 \end{aligned}\right\}$$

where $|\mu_h|$ is given by equation (B1).

If neutrons have been followed from collision to collision according to equation (4), $n_K^S(i)$ is known for each collision. The number of neutrons transmitted after exactly K collisions follows by replacing $n^S(i)$ in equations (19) by $n_K^S(i)$ and n^T by n_K^T.

Boundary conditions at extreme boundary of a cell. - Consider an infinite repetitive-slab array consisting of identical units called cells. At the extreme boundary of a cell, the leakage from the cell in any direction is compensated by leakage into the cell in the opposite direction. This necessitates determining the angular distribution at the extreme boundaries from the flux within (eqs. (B2) and (B3)) and then reflecting the angular distribution. The uncollided source neutrons must be added to $n(x_R, |\mu_h|)d\mu$ to complete the angular distribution. The first-collision distribution of these neutrons is then calculated by applying the technique of equation (B5), and so forth.

NUMERICAL EXAMPLES

Description of Slabs Studied

To illustrate the preceding development, the slab of sketch (a) was chosen with $a = b = 1$ centimeter. The total mean free path and the scattering probability per collision were respectively taken as

$\lambda^{I} = \lambda^{II} = 0.78125$ and $(\lambda/\lambda_s)^{I} = (\lambda/\lambda_s)^{II} = 8/10$. Each slab was divided into ten equal subregions ($q_1 = q_2 = 10$) giving $\Delta L_1 = \Delta L_2 = 0.1280$. A unit isotropic source plane was chosen at the interface x_0.

In the general case where $\Delta L_1 \neq \Delta L_2$, this configuration might be treated as a two-slab problem (each half separately) by using the angular distribution at x_0 to pass from one slab into the other. However, in the present case, there is the option of a single-slab treatment, which is, of course, much simpler. Both procedures were adopted for this example and gave identical results as anticipated. For the double-slab case a grid of 50 solid angles was used to pass from one slab into the other. As discussed in the text, transfer probabilities between subregions of unequal width can always be used as an alternative to the angular-distribution approach.

E-170

CY-3 back

Let P_K^T and P_K^{-T} be defined as the respective probabilities that a source neutron will be transmitted through the right or left boundaries after exactly K collisions. For example, P_0^T would be the probability of a transmission through the right boundary directly from the source. From symmetry,

$$P_K^T = P_K^{-T}$$

The multiple integrals for P_0^T and P_1^T are formulated in appendix C.

By employing the previously given values of λ and λ_s, P_0^T and P_1^T were evaluated as $P_0^T = 50.0$ and $P_1^T = 47.07$ per thousand source neutrons. Part of the contribution to P_1^T consists of neutrons that suffer the single scattering collision to the left of the source plane. The fraction of these that escape through the right boundary P_1^{LR} was evaluated as 12.3 per thousand source neutrons. In addition to the neutron flux, these values were compared with the results of the numerical method.

The block diagram for the numerical analysis, using the single-slab treatment, is given as appendix D. Twenty collisions proved sufficient to give a converged flux.

The neutron flux and transmission probabilities P_1^{LR}, P_K^T, P_K^{-T} were obtained by a Monte Carlo calculation (appendix E) considering 10,700 histories for up to 20 collisions each. The results were compared with those of the numerical method. A P_3 spherical harmonics solution (appendix F) and a P_1 diffusion-theory calculation were also performed for the total flux and were compared with the other methods.

The slab half-thickness was successively changed to 1/5 and 5 total mean free paths with the same values of λ and λ/λ_s. The numerical-method flux was compared with diffusion theory for these cases.

As a second example, the configuration of sketch (a) was chosen, but with

$$\lambda^I = 1, \left(\frac{\lambda}{\lambda_s}\right)^I = \frac{8}{10}, \lambda^{II} = 3.43, \left(\frac{\lambda}{\lambda_s}\right)^{II} = 1.0$$

and with the source plane at X_L instead of X_0. The widths of slabs I and II were taken as 2.0 and 2.0177 centimeters, respectively. By choosing $q_1 = 34$ subregions in slab I and $q_2 = 10$ subregions in slab II, equation (11) is satisfied. Thus, $\Delta L_I = \Delta L_{II} = 0.058824$. There are, of course, many other integral pairs q_1 and q_2 that could have been chosen to achieve the equality of the ΔL's.

The set of transfer probabilities $P_0, P_1, P_2, \ldots, P_{44}$ was calculated from equation (A8a). The additional set $p_1, p_2, \ldots, p_{44}$ was calculated from (A8b) in order to determine the first-collision distribution of the neutrons emanating from the source plane at X_L. The successive-collisions technique of equation (13) was applied for 28 collisions and yielded converged results. The number of neutrons transmitted after exactly K collisions past X_L and X_R was recorded in the process.

For comparison, a Monte Carlo calculation was performed for the total flux and the number of transmissions. Up to 28 collisions were allowed, and 25,000 neutron histories were followed.

Finally, the flux was obtained by solving the 44 simultaneous equations represented by equation (14).

Results

The results of the numerical and Monte Carlo methods for the symmetrical slab of sketch (a) are contained in tables I and II. Table I also includes results of the P_3 approximation. The fluxes are plotted in figures 1 and 2. Figure 2 includes a P_1 approximation for comparison with P_3.

Against the analytic values of $P_0^T = 50.0$, $P_1^T = 47.07$, and $P_1^{LR} = 12.3$ per thousand source neutrons, Monte Carlo yielded averaged values of 50.0, 47.81, and 11.97 per thousand as compared with 49.6, 47.03, and 12.18 by the numerical method. The Monte Carlo flux and

transmissions sometimes suffer an appreciable deviation from symmetry in each half of the slab (table II), but the averaged values are in good agreement with those obtained by the numerical method, which, of course, suffers no deviations from symmetry. The total leakage was 0.43406, 0.43556, and 0.43598 per source neutron per square centimeter per second by the Monte Carlo, numerical, and P_3 methods. The total absorptions, satisfying neutron conservation within 0.04 percent, were 0.56569, 0.56402, and 0.56402, respectively.

In addition to the P_1 and P_3 fluxes, figure 2 contains the results of the numerical-method solution utilizing 100 subregions instead of 20, as presented in figure 1. The finer mesh was chosen to test the accuracy of lumping the scattered neutrons at the center of each subregion and to acquire a more detailed variation of flux than appears in figure 1. When averaged over each subregion of figure 1, the numerical flux differs by a small fraction of a percent from the 20-subdivision case, implying a negligible lumping error. The same is true for the P_K^T's, K = 0,1, . . ., 19. Thus, for practical purposes the 100-subregion case represents a precise solution of integral equation (10) and hence the transport equation, in the sense that further subdivisions would yield negligible changes and that the numerical method has exactly treated the angular dependence.

Utilizing the same total and scattering mean free paths as before, figures 3 and 4 contain numerical-method flux plots for slabs of 1/5 and 5 total mean free paths half-thickness, respectively, from the source plane to either boundary. The diffusion-theory flux is plotted for comparison.

Figure 3 shows the agreement between the numerical method and diffusion theory to be poor everywhere, whereas in figure 4 the agreement is excellent beyond $2\frac{1}{2}$ mean free paths from the source.

A total of 10,700 Monte Carlo neutron histories required about 2 hours of IBM 653 machine operating time as compared with 3 minutes for the numerical method. Sketch (a), worked as a double-slab problem, required about 4 minutes per slab per interface crossing. Twenty collisions were followed within each slab. Thirty minutes machine time corresponding to eight interface crossings yielded results identical to those listed in table I.

The numerical and Monte Carlo results for the second example (two-region unsymmetrical slab) are listed respectively in tables III and IV, and the fluxes are plotted in figure 5. Table III shows that 28 collisions proved sufficient to obtain the neutron flux accurate to the fourth decimal place in comparison with the solution of the 44 simultaneous equations for the neutron flux.

Figure 5 shows that the numerical flux plots into a smooth curve about which the Monte Carlo solution oscillates. The reasonably close agreement implies a check on the correctness of the numerical solution. Identical remarks apply to the transmission probabilities in tables III and IV.

The numerical-method leakage through the X_L and X_R boundaries was 0.68969 and 0.061656 per source neutron to give a total-leakage probability of 0.75135 per source neutron. The respective Monte Carlo values are 0.694384, 0.060358, and 0.75474. The total absorption per source neutron is 0.248628 by the numerical method and 0.245178 by the Monte Carlo calculation and thus checks neutron conservation.

Following 28 successive collisions numerically required about 30 minutes machine operating time as compared with 15 minutes machine time in solving the 44 simultaneous equations. Twenty-five thousand Monte Carlo histories required about 10 hours.

Discussion of Results

The 100-subregion case of the slab of sketch (a), as opposed to the 20-subregion case, yielded virtually identical results for all the flux and transmission values. From this, it is concluded that the error introduced by lumping the scattered neutrons at the center of a subregion was negligible for this problem.

Anticipated qualitative features are confirmed in figures 2, 3, and 4. The readily obtained numerical result is in excellent agreement with P_3 beyond 1 mean free path from the source and with diffusion theory beyond 2.5 mean free paths. From the source to about 1/5 of a mean free path, the agreement of P_3 and P_1 with the numerical method is poor and becomes worse, in general, as the source plane is approached. In this vicinity, a proper treatment by transport theory requires a large number of spherical harmonic terms to account for the large forward bias in the net neutron current.

The quantity $1/\lambda \equiv \Sigma$ was chosen such that $P_0^T = 50.0/1000$, and therefore $\Sigma \cong 1.280$. This value of Σ was obtained by visual interpolation from a set of curves given in reference 5.

The simultaneous-equation approach of equation (14) proved best in the unsymmetrical-slab case or second example. This solution represents the flux that would be obtained by following an infinite number of

successive collisions according to equation (13). This approach, therefore, represents the solution to the problem.

Lewis Research Center
National Aeronautics and Space Administration
Cleveland, Ohio, December 11, 1958

E-170

APPENDIX A

CALCULATION OF TRANSFER PROBABILITIES AND LUMPING ERROR

A neutron is scattered or born isotropically at x' in dx' in sketch (b). Denote by $P^T(x',x)$ the probability that it will pass directly through the infinite plane at x without suffering a collision.

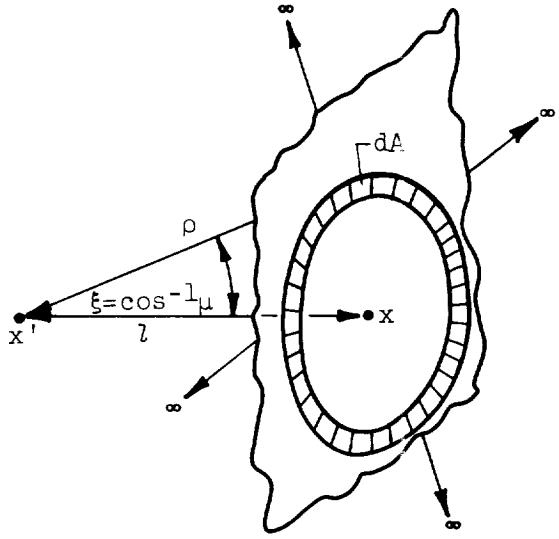

Sketch (t)

The probability that it scatters with direction cosine μ in $d\mu$ is $\frac{1}{2}\,d\mu$ (appendix E). The probability of traversing a distance ρ without a collision is $e^{-\rho/\lambda}$. Summing over-all angles to the right of the source gives $P^T(x',x)$.

$$P^T(x',x) = \frac{1}{2}\int_0^1 d\mu\; e^{-(x-x')/\lambda\mu} \qquad x > x' \qquad \text{(A1)}$$

The probability that the next collision occurs in dx about x is

$$P(x',x)dx = \lim_{\Delta x \to 0} P^T(x',x) - P^T(x'\ x+\Delta x)$$

$$= \lim_{\Delta x \to 0} \frac{1}{2}\int_0^1 d\mu\; e^{-(x-x')/\lambda\mu}\,(1 - e^{-\Delta x/\lambda\mu})$$

$$= \frac{1}{2}\int_0^1 d\mu\; e^{-(x,x')/\lambda\mu}\,\frac{d\xi}{\lambda\mu}$$

By letting $t = \frac{x - x'}{\lambda\mu}$ and $l \equiv \frac{x - x'}{\lambda}$, this expression becomes

$$P(x',x)dx = \frac{dx}{2\lambda} \int_{(x-x')/\lambda}^{\infty} \frac{e^{-t}}{t}\, dt \qquad x > x' \tag{A2}$$

and (A1) becomes

$$P^T(l) = \frac{l}{2} \int_{l}^{\infty} \frac{e^{-t}}{t^2}\, dt \tag{A3}$$

Equation (A2) represents the kernel of integral equation (10) when $x > x'$ and is the well-known exponential integral. If $x < x'$, the only change is to replace $x - x'$ by $x' - x$. The symbol l is the number of mean free paths in $|x - x'|$ centimeters.

Integrating by parts gives

$$P^T(l) = \frac{1}{2} e^{-l} - \frac{l}{2} \int_{l}^{\infty} \frac{e^{-t}}{t}\, dt \tag{A4}$$

and

$$I_l \equiv \int_{l}^{\infty} \frac{e^{-t}}{t}\, dt = \int_{l}^{15} \left[\frac{1}{t} + \sum_{n=1}^{\infty} \frac{(-1)^n t^{n-1}}{n!}\right] dt + \int_{15}^{\infty} \frac{e^{-t}}{t}\, dt$$

The value of the second term is given in Jahnke and Embde as 1.92×10^{-8}. Integrating this series term by term gives

$$I_l = 1.92 \times 10^{-8} + \ln 15 + \sum_{n=1}^{\infty} \frac{(-1)^n 15^n}{n!\,n} - \ln l + \sum_{n=1}^{\infty} \frac{(-1)^{n+1} l^n}{n!\,n} \tag{A5}$$

The first three terms are lumped into a single constant. The result is -0.57721560. Equation (A4) becomes

$$P^T(l) = 0.5 - 0.21139220\, l + \frac{1}{2}\, l \ln l - \frac{1}{2} \sum_{n=1}^{\infty} \frac{(-1)^{n+1} l^{n+1}}{(n+1)!\,n} \tag{A6}$$

This expression is the probability that a neutron scattered or born isotropically at x' is transmitted through a boundary l mean free paths away with no intervening collisions.

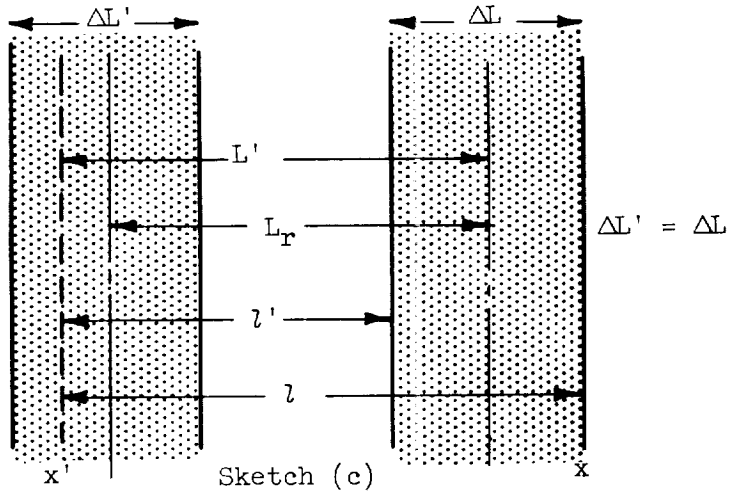

Sketch (c)

By referring to sketch (c), the transfer probability between the two shaded subregions is computed as follows:

All neutrons scattered in $\Delta L'$ are lumped at x' inside $\Delta L'$; x' is ordinarily chosen at the center of $\Delta L'$. This is not an essential choice, but it is a convenient one. The subregions have been taken sufficiently small so that the lumping error can be neglected.

The quantity L' is the distance in mean free paths from the source plane to the center of ΔL; L_r is the distance from the center of $\Delta L'$ to the center of ΔL. The probability that a neutron scattered in $\Delta L'$ will make its next collision anywhere in ΔL is given by

$$P(l',l) = P^T(l') - P^T(l) \qquad \text{(A7)}$$

But $l' = L' - \frac{\Delta L}{2}$ and $l = L' + \frac{\Delta L}{2}$. Substituting from equation (A6), (A7) becomes

$$P(L',\Delta L) = 0.21139220\ \Delta L + \frac{1}{2}\left(L' - \frac{\Delta L}{2}\right)\ln\left(L' - \frac{\Delta L}{2}\right) - \frac{1}{2}\left(L' + \frac{\Delta L}{2}\right)\ln\left(L' + \frac{\Delta L}{2}\right) +$$

$$\frac{1}{2}\sum_{n=1}^{\infty} \frac{(-1)^{n+1}}{(n+1)!n}\left[\left(L' + \frac{\Delta L}{2}\right)^{n+1} - \left(L' - \frac{\Delta L}{2}\right)^{n+1}\right] \qquad \text{(A8)}$$

$P(L',\Delta L)$ is the transfer probability from a source plane into a subregion of width ΔL whose center lies L' mean free paths away from the source plane.

The source plane is ordinarily taken at the center of a subregion. Then,

$$\left.\begin{aligned} L' \equiv L_r &= r\,\Delta L \\ P(L_r,\Delta L) &\equiv P_r \end{aligned}\right\} r = 1,2\ \ldots,\ (q-1) \qquad \text{(A8a)}$$

If a source plane exists at the boundary of a subregion,

$$\left.\begin{aligned} L' \equiv l_r &= \left(r - \tfrac{1}{2}\right)\Delta L \\ P(l_r,\Delta L) &\equiv p_r \end{aligned}\right\} \qquad \text{(A8b)}$$

The probability that a neutron will make its next collision in the subregion in which it scattered is given as

$$P_0 = 1 - 2P^T\left(\frac{\Delta L}{2}\right) = 0.21139220\,\Delta L - \frac{\Delta L}{2}\ln\frac{\Delta L}{2} + \sum_{n=1}^{\infty}\frac{(-1)^{n+1}}{(n+1)!\,n}\left(\frac{\Delta L}{2}\right)^{n+1} \qquad \text{(A9)}$$

Transfer Probabilities Between Unequal Subregions

Suppose that $\Delta L' \equiv \Delta L_I$ lies in medium I and $\Delta L \equiv \Delta L_{II}$ lies in medium II. It can be proven that, for slab geometry, the transfer probability still depends on the total distance in mean free paths from the source plane in ΔL_I to the collision center of ΔL_{II}. From sketch (d),

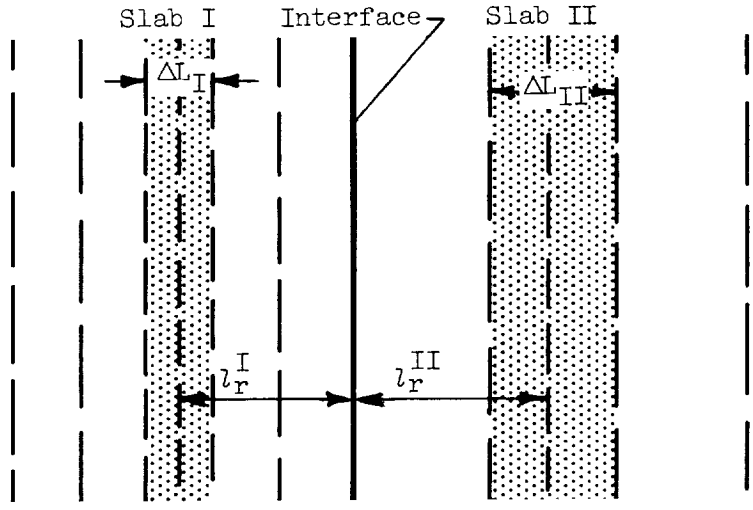

Sketch (d)

$$\left.\begin{aligned} L' &= l_r^I + l_r^{II} \\ l_r^I &= \left(r_1 - \tfrac{1}{2}\right)\Delta L_I \\ l_r^{II} &= \left(r_2 - \tfrac{1}{2}\right)\Delta L_{II} \end{aligned}\right\} r_1, r_2, = 1,2, \ldots \qquad \text{(A10)}$$

Equation (A8) now reads:

$$P(\Delta L_I, \Delta L_{II}) = 0.21139220\ \Delta L_{II} + \tfrac{1}{2}\left(l_r^I + l_r^{II} - \frac{\Delta L_{II}}{2}\right)\ln\left(l_r^I + l_r^{II} - \frac{\Delta L_{II}}{2}\right) -$$

$$\tfrac{1}{2}\left(l_r^I + l_r^{II} + \frac{\Delta L_{II}}{2}\right)\ln\left(l_r^I + l_r^{II} + \frac{\Delta L_{II}}{2}\right) +$$

$$\tfrac{1}{2}\sum_{n=1}^{\infty}\frac{(-1)^{n+1}}{(n+1)!n}\left[\left(l_r^I + l_r^{II} + \frac{\Delta L_{II}}{2}\right)^{n+1} - \left(l_r^I + l_r^{II} - \frac{\Delta L_{II}}{2}\right)^{n+1}\right] \qquad \text{(A11)}$$

where l_r^I and l_r^{II} are given by (A10). Equation (A11) is used to calculate transfer probabilities between unequal subregions.

E-170

Lumping Error

Again, in sketch (c) the lumping error per collision ϵ arises because neutrons scattered anywhere in $\Delta L'$ are lumped at a source plane at the center of $\Delta L'$. If $S(L')dL'$ is the true source distribution inside $\Delta L'$, where dL' is of infinitesimal width, the lumping error for the transfer probability $P(L_r,\Delta L)$ is

$$\epsilon = \left| \frac{\displaystyle\int_{L_r - \frac{\Delta L}{2}}^{L_r + \frac{\Delta L}{2}} S(L')P(L',\Delta L)dL'}{\displaystyle\int_{L_r - \frac{\Delta L}{2}}^{L_r + \frac{\Delta L}{2}} S(L')dL'} - P(L_r,\Delta L) \right| \qquad \text{(A12)}$$

Equation (A12) implies that if all neutrons inside $\Delta L'$ were actually scattered from a source plane at its center, the lumping error for $P(L_r,\Delta L)$ would be zero. This is verified by substituting $S(L') = S\delta(L' - L_r)$ into (A12).

The maximum possible lumping error that could arise would occur if all neutrons were scattered in $\Delta L'$ at either of the two boundaries of $\Delta L'$. Then,

$$S(L')dL' = S\delta\left(L' - L_r - \frac{\Delta L}{2}\right)dL' \qquad (\text{for } \epsilon_a)$$

or

$$S(L')dL' = S\delta\left(L' - L_r + \frac{\Delta L}{2}\right)dL' \qquad (\text{for } \epsilon_b)$$

Then

$$\epsilon_a = \left| P\left(L_r + \frac{\Delta L}{2}, \Delta L\right) - P(L_r, \Delta L) \right|$$

$$\epsilon_b = \left| P\left(L_r - \frac{\Delta L}{2}, \Delta L\right) - P(L_r, \Delta L) \right|$$

For P_0, for example, the maximum possible error is

$$\epsilon_{max} = P_0 - p_1 = \text{eq. (A9)} - \text{eq. (A8b)} = \frac{\Delta L}{2} \ln 2 + \sum_{n=1}^{\infty} \frac{(-1)^{n+1}(\Delta L)^{n+1}}{(n+1)!\,n}\left(\frac{1}{2^{n+1}} - \frac{1}{2}\right)$$

In actual practice the error will be considerably smaller than this because neutrons will be distributed throughout $\Delta L'$.

Insight into the magnitude of the lumping error may be gained by writing $S(L') = \zeta L' + \eta$ in equation (A12). This accurately approximates the correct but unspecified source distribution in $\Delta L'$, provided $\Delta L'$ is small. The quantity η is chosen so as to normalize the source distribution in $\Delta L'$, while ζ remains an unknown parameter unless the source distribution is specified. The integration in (A12) can then be performed with the result being indicated as $f(L,\Delta L,\zeta)$. Thus,

$$\epsilon(\zeta, L_r, \Delta L) = f(L_r, \Delta L, \zeta) - P(L_E, \Delta L)$$

where L_E has been written for L_r in the $P(L_r,\Delta L)$ term of equation (A12). By setting $\epsilon = 0$ and solving this complicated equation for L_E, the exact location within $\Delta L'$ where all the scattered neutrons can be lumped with zero error is obtained for a given ζ, L, and ΔL. This point will rarely coincide with the center.

APPENDIX B

ANGULAR DISTRIBUTION AND FIRST-COLLISION DISTRIBUTION DUE TO AN ANISOTROPIC SOURCE PLANE

Angular Distribution

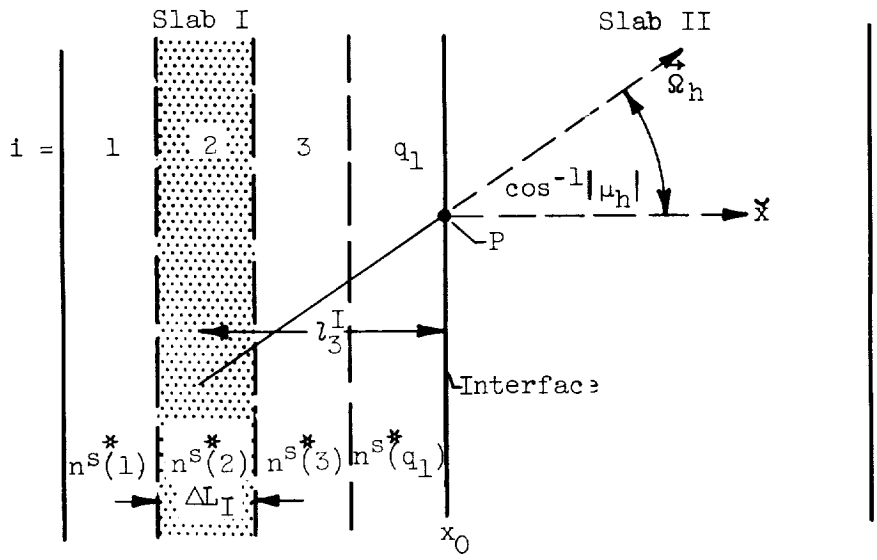

Sketch (e)

The angular distribution at the interface of neutrons entering slab II from slab I is computed from the known number of scattering hits $n^s(i)$ in slab I.

In sketch (e), $\vec{\Omega}_h$ is a unit vector in the direction of the neutron velocity that is specified by the cosine of the angle between $\vec{\Omega}_h$ and the x axis; that is, $\mu_h = \vec{\Omega}_h \cdot \vec{x}$. The vector $\vec{\Omega}_h$ can be considered as the radius vector of a unit sphere about the point P as its center.

The surface of the hemisphere to the right of the interface is divided into a grid of g strips of equal areas formed by rotating $\vec{\Omega}_h$ about the x axis for h = 1,2, . . ., g. Then,

$$d\mu = \frac{1}{g} \qquad |\mu_h| = |\mu_{h-1}| + \frac{1}{g}\left(1 - \frac{1}{2}\delta_{h,1}\right)$$
$$\mu_0 \equiv 0 \qquad h = 1,2, \ldots, g \tag{B1}$$

where $\delta_{h,1}$ is the Kronecker delta. Thus, if $g = 50$, for example, $d\mu = 0.02$ and $\mu_1 = 0.01$, $\mu_2 = 0.03$, $\mu_3 = 0.05$, . . . $\mu_{50} = 0.99$.

The fraction of neutrons scattered into $d\mu$ is $\frac{1}{2}\,d\mu$. The fraction that reaches the interface from the scattering center in subregion i without further collisions and with direction cosine $|\mu_h|$ is $e^{-l^{I}_{q_1+1-i}/|\mu_h|}$. Thus,

$$n(x_0,|\mu_h|)d\mu = \sum_{i=1}^{q_1} n^s(i)\,\tfrac{1}{2}\,d\mu\; e^{-l^{I}_{q_1+1-i}/|\mu_h|} \qquad \mu_h > 0$$

$$l^{I}_{q_1+1-i} = \left[(q_1 + 1 - i) - \tfrac{1}{2}\right]\Delta L_I \qquad \text{(B2)}$$

Similarly,

$$n(x_0,|\mu_h|)d\mu = \sum_{i=q_1+1}^{q} n^s(i)\,\tfrac{1}{2}\,d\mu\; e^{-l^{II}_{i-q_1}/|\mu_h|} \qquad \mu_h < 0$$

$$l^{II}_{i-q_1} = \left[(i - q_1) - \tfrac{1}{2}\right]\Delta L_{II} \qquad \text{(B3)}$$

Equation (B2) is the angular distribution entering the second slab due to the flux in the first, and (B3) is the converse. It should be noted that the angular distribution is not isotropic.

First-Collision Distribution in Second Slab Due to Angular Distribution

Define δ^{I}_{h} as the probability that a neutron with direction cosine μ_h will pass through a single subregion of slab I without a collision.

$$\left.\begin{aligned} \delta^{I}_{h} &\equiv e^{-\Delta L_I/|\mu_h|} \\ \delta^{II}_{h} &\equiv e^{-\Delta L_{II}/|\mu_h|} \end{aligned}\right\} \qquad \text{(B4)}$$

The quantity $1 - \delta_h$ is the probability that a neutron with direction cosine μ_h will collide within a single subregion.

The number scattered from the first collision in each subregion i of the second medium is therefore

$$n_1^s(i) = \left(\frac{\lambda}{\lambda_s}\right)^{II} \sum_{h=1}^{g} n(x_0,\mu_h)d\mu(\delta_h^{II})^{i-q_1-1}\,(1 - \delta_h^{II}) \qquad \mu_h > 0 \qquad \text{(B5)}$$

$$i = q_1+1, q_1+2, \ldots, q$$

From slab II into slab I,

$$n_1^s(i) = \left(\frac{\lambda}{\lambda_s}\right)^{I} \sum_{h=1}^{g} n(x_0,|\mu_h|)d\mu(\delta_h^{I})^{q_1-i}\,(1 - \delta_h^{I}) \qquad \mu_h < 0 \qquad \text{(B6)}$$

$$i = 1,2, \ldots, q_1$$

The factor $(\delta_h)^{q_1-i}(1 - \delta_h^I)$ gives the fraction of the $n(x_0,\mu_h)d\mu$ interface neutrons that pass through $q_1 - i$ subregions of medium I without a collision and that collide in the next subregion.

APPENDIX C

EVALUATION OF INTEGRALS FOR PROBABILITY OF TRANSMISSION WITH NO COLLISION AND ONE COLLISION

The quantity P_0^T is equivalent to equation (A3). For the slab of sketch (a), $l = a/\lambda = 1/\lambda$, since a has been chosen to be 1 centimeter; P_0^T was arbitrarily chosen as 50.0/1000; λ was determined so as to give this value, and turned out to be approximately 0.78125 (ref. 5).

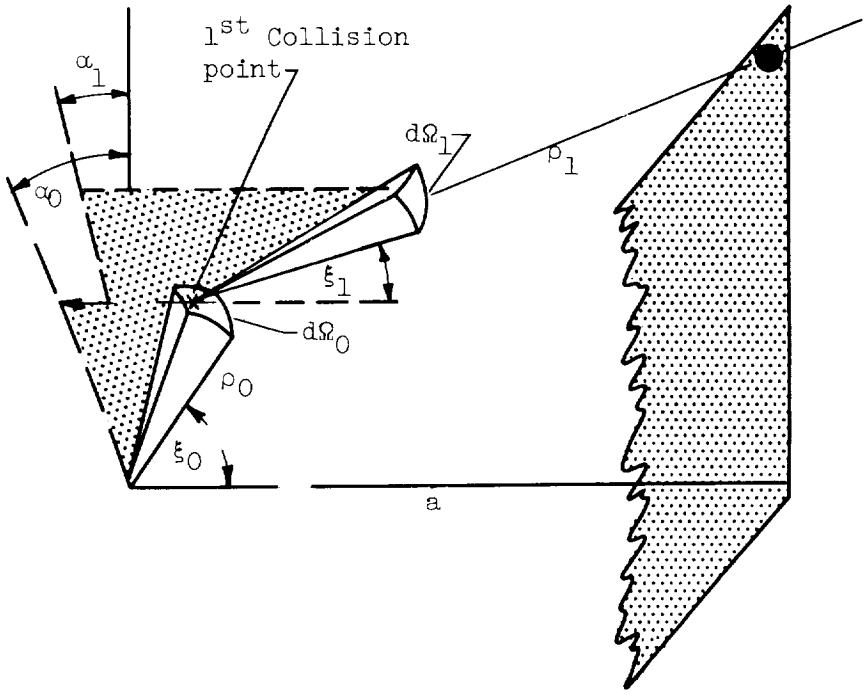

Sketch (f)

To evaluate P_1^T, consider sketch (f). Let P_1^{RR} and P_1^{LR} denote the respective probabilities of a source neutron suffering its first collision to the right or left of the origin and then escaping through the right-hand boundary. Then

$$P_1^T = P_1^{RR} + P_1^{LR} \tag{C1}$$

To evaluate P_1^{RR}, for example, write the expression for the number of neutrons per square centimeter per second $(N^T(\Omega_0,\Omega_1,\rho_0,\rho_1)d\Omega_0,d\Omega_1,d\rho_0)$ born into solid angle $d\Omega_0$, scattered into $d\Omega_1$ at a radius ρ_0 from

the origin, and traveling the remaining distance ρ_1 to the right-hand boundary without a subsequent collision. If a total of N neutrons per square centimeter per second are isotropically born from the source,

$$N^T(\Omega_0,\Omega_1,\rho_0,\rho_1)d\Omega_0 d\Omega_1 d\rho_0 = N \frac{d\Omega_0}{4\pi} e^{-\rho_0/\lambda} \frac{d\rho_0}{\lambda_s} \frac{d\Omega_1}{4\pi} e^{-\rho_1/\lambda}$$

where $d\Omega = - d\mu\, d\alpha$, $\rho_0 = \frac{x_1}{\mu_0}$, $\rho_1 = \frac{a - x_1}{\mu_1}$, and $\mu = \cos \xi$. By summing up all Ω_0's, Ω_1's, and x_1's, P_1^{RR} is obtained:

$$P_1^{RR} = \int_{x_1=0}^{a} \int_{\mu_0=0}^{1} \int_{\alpha_0=0}^{2\pi} d\alpha_0 d\mu_0 dx_1 \frac{1}{4\pi\lambda_s} \frac{e^{-\frac{x_1}{\mu_0\lambda}}}{\mu_0} \int_{\mu_1=0}^{1} \int_{\alpha_1=0}^{2\pi} d\alpha_1 d\mu_1 \frac{1}{4\pi} e^{-\frac{a-x_1}{\mu_1\lambda}}$$

Similarly,

$$P_1^{LR} = -\int_{x_1=-a}^{0} \int_{\mu_0=0}^{-1} \int_{\alpha_0=0}^{2\pi} d\alpha_0 d\mu_0 dx_1 \frac{1}{4\pi\lambda_s} \frac{e^{-\frac{x_1}{\mu_0\lambda}}}{\mu_0} \int_{\mu_1=0}^{1} \int_{\alpha_1=0}^{2\pi} d\alpha_1 d\mu_1 \frac{1}{4\pi} e^{-\frac{a-x_1}{\mu_1\lambda}}$$

Integrating these expressions over α_0, α_1, and x_1 gives

$$\left.\begin{aligned} P_1^{RR} &= \frac{a^2}{4\lambda\lambda_s} \int_0^{\lambda/a} \int_0^{\lambda/a} d\nu_0 d\nu_1 \left(\frac{e^{-1/\nu_1} - e^{-1/\nu_0}}{1 - \nu_0/\nu_1} \right) \\ P_1^{LR} &= \frac{a^2}{4\lambda\lambda_s} \int_0^{\lambda/a} \int_0^{\lambda/a} d\nu_0 d\nu_1 \, e^{1/\nu_1} \left[\frac{1 - e^{-\left(\frac{1}{\nu_0} + \frac{1}{\nu_1}\right)}}{1 + \nu_0/\nu_1} \right] \end{aligned}\right\} \quad (C2)$$

Integrals (C2) were evaluated on the IBM 653 by using the definition of double integrals and a value of λ/λ_s equal to 0.8. The results are:

$$P^{RR} = \frac{34.76}{1000} \quad \text{and} \quad P_1^{LR} = \frac{12.31}{1000}$$

Thus, from equation (C1),

$$P_1^T = \frac{47.07}{1000}$$

The values

$$P_0^T = \frac{50.0}{1000}, \quad P_1^T = \frac{47.07}{1000}, \quad P_1^{LR} = \frac{12.31}{1000} \tag{C3}$$

were to be checked by the Monte Carlo and numerical methods.

APPENDIX D

NUMERICAL TREATMENT OF SLAB OF SKETCH (a)

The values of the constants (see p. 12) are $q = 20$, $a = 1$ centimeter, $\lambda = 0.78125$, $\lambda/\lambda_s = 0.8$, and $S_{x_0} = 1$ neutron per square centimeter per second. Thus, $\Delta L = 0.1280$. In evaluating the transfer probabilities, fifteen terms of the series in equations (A8) and (A9) were used, so that extreme accuracy was obtained for $\Delta L = 0.1280$.

The accompanying block diagram summarizes the main points of the illustrative slab calculation but omits the steps for obtaining P_1^{LR}. From $\sum_{K=1}^{20} n_K^s(i) \equiv n^s(i)$, the average flux in i was calculated by equation (6).

NUMERICAL-METHOD BLOCK DIAGRAM

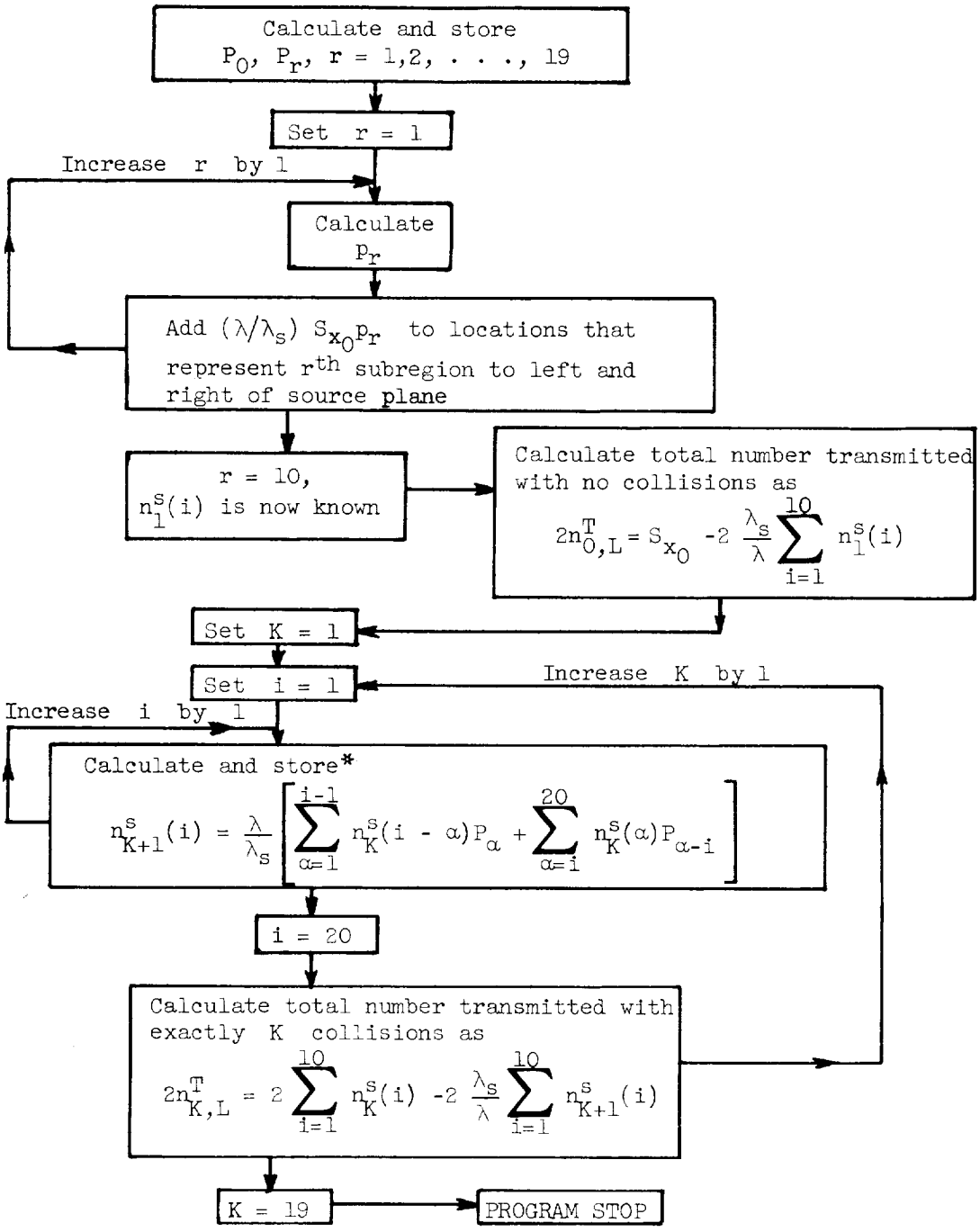

*Sixty locations are used for this purpose: 20 locations to accumulate the number of scattering hits in each subregion for all collisions, 20 to store the number from the previous collision, $n_K^s(i)$, and 20 as the working area for $n^s_{K+1}(i)$.

APPENDIX E

MONTE CARLO CALCULATION OF NEUTRON FLUX AND TRANSMISSION INTEGRALS

Sketch (g) shows one of the symmetrical halves of the slab of sketch (a). The purpose of the Monte Carlo calculation was to obtain the total

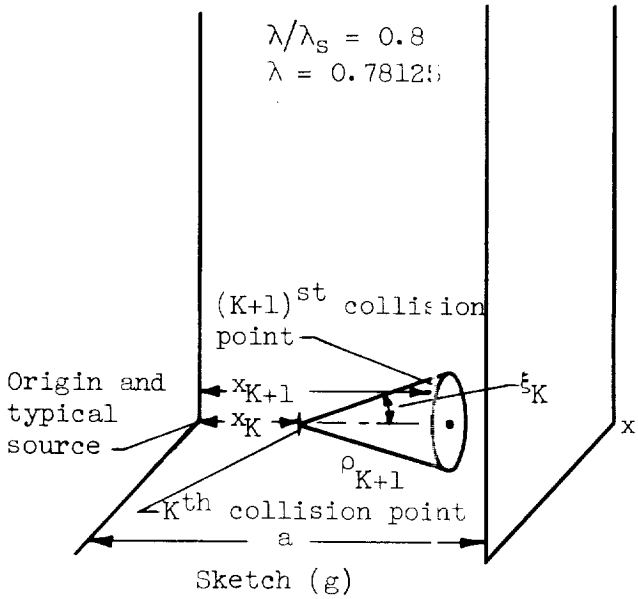

Sketch (g)

neutron flux and transmission integrals P_0^T, P_1^T, and P_1^{LR} (whose values are given by eq. (C3)) and to compare them with the values and time taken by the numerical method. The probabilities P_K^T, K = 2,3, . . ., 19 were also recorded and compared, though not analytically evaluated because of the complexities. The fact that these multiple-scattering transmission integrals are so readily obtainable by Monte Carlo demonstrates the utility of following individual neutron histories for thin slabs.

The complete slab was divided into 20 subregions, and the total number of scattering hits (proportional to the average flux) was recorded in each. In following individual histories, all collisions were treated as scatterings by the well-known technique of weighting the colliding neutron by $(1 - \Sigma_a/\Sigma)$ per collision. A neutron leaving the slab from the K^{th} collision was recorded in the T_K or $T_{\overline{K}}$ location of the machine, depending on the boundary through which it escaped.

To achieve accurate results, 10,700 histories were followed.[1] By averaging corresponding fluxes and transmissions in both halves, the equivalent of 10,700 case histories in each half is obtained. A Monte Carlo treatment of this slab involves the following:

(1) Choosing random numbers:

A pseudo random number $Rn+1$ was generated by taking $Rn+1 = \rho Rn$ where $\rho = 9,677,214,091$ and $R_0 = 6,250,739,481$ and by retaining only the right ten digits in the product. The extreme right digit always ends with a 1, but nine-digit accuracy is more than sufficient. The 1 prevents degeneracy from occurring too quickly.

(2) Choosing direction of travel after isotropic scattering collision in laboratory system:

Because the direction of travel after an isotropic scattering collision is unrelated to any previous direction, the x-axis can always be chosen as the fixed reference or initial direction. The scattering angle thereby formed is denoted by ξ and its cosine by μ.

From sketch (h), the probability distribution function for a neutron passing through the shaded area dA is

$$p(\xi)d\xi = dA/4\pi$$

$$= \frac{1}{2} \sin \xi \, d\xi$$

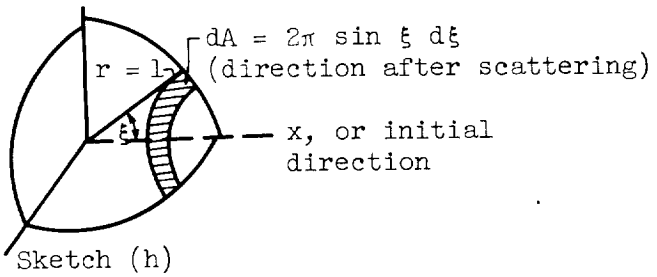

Sketch (h)

The cumulative distribution function is $\int_0^{\xi} p(\xi')d\xi'$ and is set equal to a random number R_1 to give

$$\cos \xi = \mu = 1 - 2R_1 \qquad \text{(E1)}$$

---

[1] The standard deviation of P_0^T, for example, is $\sigma = \sqrt{np(1-p)} = \sqrt{10,700}\sqrt{0.05 \times 0.95}$. Thus, in the Monte Carlo calculation, $P_0^T = \frac{50}{1000} \pm \frac{0.6745\sigma}{10,700} = \frac{50.0 \pm 1.35}{1000}$ with 50-percent expectancy.

Thus, to pick from an isotropic distribution in the laboratory system, a random number is chosen, and equation (E1) is applied. Picking an aximuthal angle is unnecessary for this slab problem.

(3) Picking distance of travel to next collision:

The probability distribution function for a neutron traveling a distance ρ without a collision and then colliding in $d\rho$ is $p(\rho)d\rho = e^{-\rho/\lambda}\frac{d\rho}{\lambda}$. The cumulative distribution function is $\int_0^\rho p(\rho')d\rho'$, and equating to a random number gives

$$\rho = -\lambda \ln (1 - R_2') = -\lambda \ln R_2 \qquad (E2)$$

(4) From sketch (g), the penetration distance is:

$$X_{K+1} = X_K + \rho_{K+1}\mu_K \qquad (E3)$$

where X_K is the X coordinate of the previous or K^{th} collision.

The Monte Carlo problem was programmed according to the block diagram given on the next page. After following 10,700 histories for up to 20 collisions per history, the total number of scattering hits $n^S(i)$ in each subregion i was punched out in addition to the transmission probabilities P_K^T, P_K^{-T}, P_1^{LR}, K = 0, 1, . . ., 19. Then, the average flux in i was calculated by

$$\bar{\Phi}(i) = n^S(i)/(\Sigma_s \Delta X \times 10,700)$$

where ΔX is the thickness of subregion i in centimeters and 10,700 is the normalizing factor. The number of neutrons transmitted was also normalized to one source neutron by dividing by 10,700.

MONTE CARLO BLOCK DIAGRAM

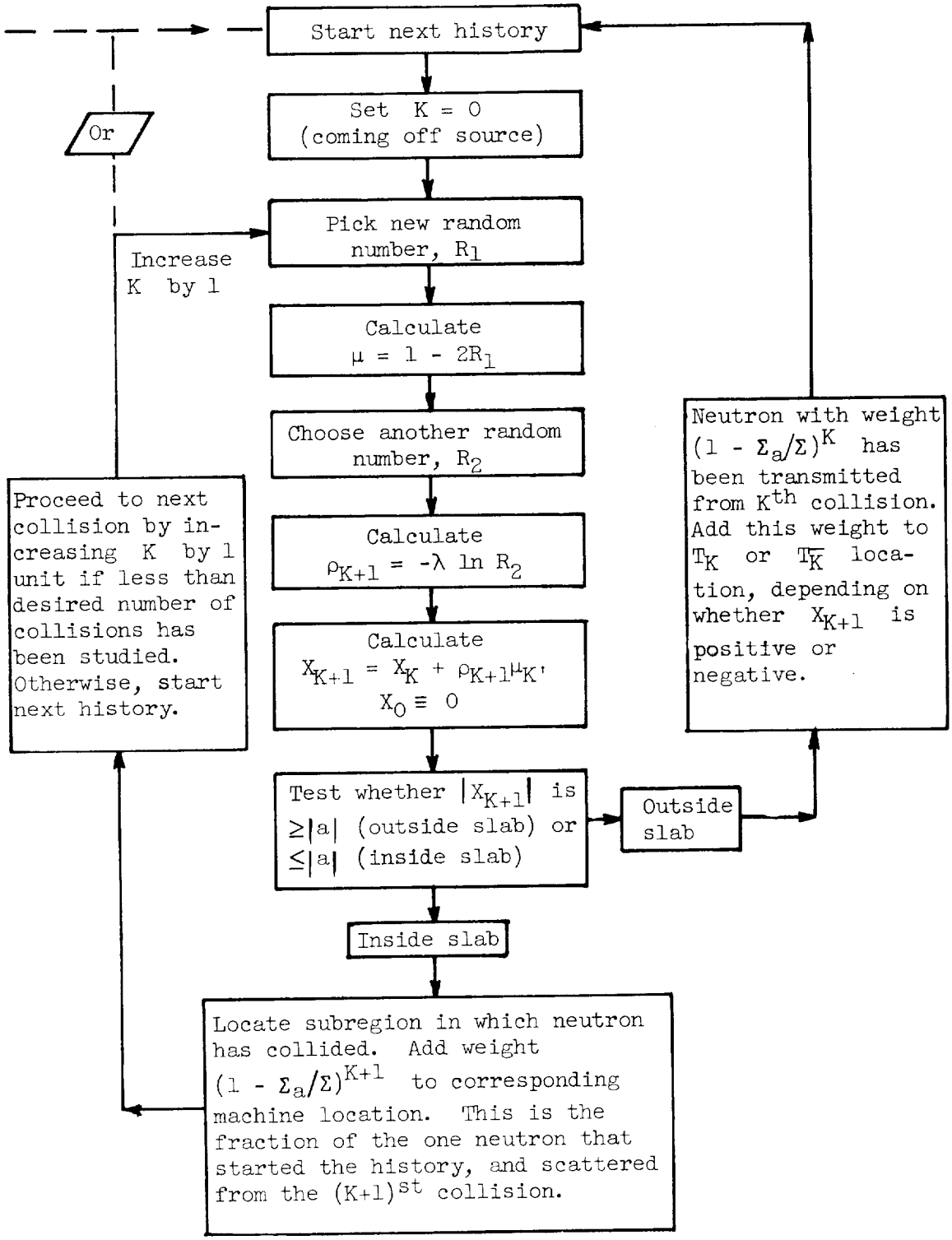

APPENDIX F

P_3 SPHERICAL HARMONICS SOLUTION

The P_3 approximation in the Legendre series expansion of the transport flux,

$$F(x,\mu) \cong \sum_{l=0}^{3} \frac{2l+1}{2} F_l(x) P_l(\mu)$$

$$F_l(x) = \int_{-1}^{1} F(x,\mu) P_l(\mu) d\mu$$

gives rise to four simultaneous differential equations for the total neutron flux $F_0(x)$ when substituted into the transport equation (ref. 1). For isotropic scattering in the laboratory system and a distributed constant isotropic source S, these equations are:

$$\left.\begin{aligned} F_1'(x) + b_0 F_0(x) - S &= 0 \\ F_0'(x) + 2F_2'(x) + 3b_1 F_1(x) &= 0 \\ 2F_1'(x) + 3F_3'(x) + 5b_1 F_2(x) &= 0 \\ 3F_2'(x) + 7b_1 F_3(x) &= 0 \end{aligned}\right\} \qquad (F1)$$

The net neutron diffusion current is $F_1(x)$, while $F_2(x)$ and $F_3(x)$ are higher order fluxes and currents; b_1 is the macroscopic total cross section and b_0 the macroscopic absorption cross section. An identical set of equations holds for another region, say A, except that S_A neutrons per cubic centimeter per second replaces S and the b's are replaced by a's.

Consider sketch (i). As discussed in reference 1, the source plane is treated as a vacuum region of width $2x_1$, which is eventually allowed to approach zero with $2x_1 S_A$ approaching 1 neutron per square centimeter per second. Since region A is vacuum, $a_0 = a_1 = 0$.

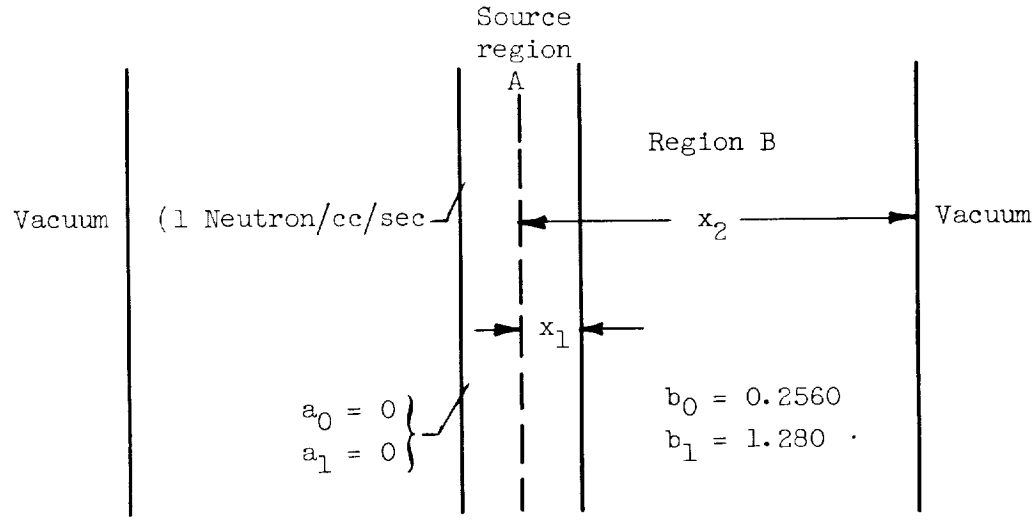

Sketch (i). - Slab of sketch (a) by spherical harmonics.

The solution of equations (F1) for regions A and B is:

$$\left.\begin{aligned} F_0^A(x) &= A_0 & F_0 &= \sum_{\nu=1}^{4} B_\nu e^{\beta_\nu |x|} \\ F_1^A(x) &= S_A x + A_1 & F_1 &= \sum_{\nu=1}^{4} \gamma_\nu B_\nu e^{\beta_\nu |x|} \\ F_2^A(x) &= A_2 & F_2 &= \sum_{\nu=1}^{4} \delta_\nu B_\nu e^{\beta_\nu |x|} \\ F_3^A(x) &= -(2/3)\, S_A x + A_3 & F_3 &= \sum_{\nu=1}^{4} \lambda_\nu B_\nu e^{\beta_\nu |x|} \end{aligned}\right\} \quad (F2)$$

where A and B are arbitrary constants. Also

$$\left.\begin{aligned} &\gamma_\nu = -\frac{b_0}{\beta_\nu} \qquad \delta_\nu = \frac{3b_0b_1}{2\beta_\nu^2} - \frac{1}{2} \qquad \lambda_\nu = \frac{3}{14b_1}\left(\beta_\nu - \frac{3b_0b_1}{\beta_\nu}\right) \\ &\beta_\nu^4 - \varkappa_1\beta_\nu^2 + \varkappa_2 = 0\,; \quad \varkappa_1 = 3b_0b_1 + \frac{35}{9}b_1^2 + \frac{28}{9}b_0b_1\,; \quad \varkappa_2 = \frac{35}{3}b_0b_1^3 \end{aligned}\right\} \quad (F3)$$

The boundary conditions are (ref. 6):

At $x = 0$,

$$\left.\begin{aligned} F_1^A(0) &= 0 \\ F_3^A(0) &= 0 \end{aligned}\right\} \qquad \text{(F4)}$$

At $x = x_1$,

$$F_m^A(x_1) = F_m^B(x_1) \qquad m = 0,1,2,3 \qquad \text{(F5)}$$

At $x = x_2$,

$$\left.\begin{aligned} \int_0^{-1} F(x_2,\mu)P_1(\mu)d\mu &= 0 \\ \int_0^{-1} F(x_2,\mu)P_3(\mu)d\mu &= 0 \end{aligned}\right\} \qquad \text{(F6)}$$

Equation (F4) is implied from the requirement that no net flow of neutrons occurs in any direction across the plane of symmetry. Equation (F5) expresses the continuity of the transport flux in any direction across the interface, and (F6) is the set of boundary conditions proposed by Marshak (in ref. 1) to approximate the rigorous boundary condition that no neutrons reenter the slab from the vacuum; that is, $F(x_2,\mu) \equiv 0, \mu < 0$. In addition, the symmetry condition $F(x,\mu) = F(-x,-\mu)$ must be satisfied.

From equation (F3),

$$\beta_{1,2,3,4} = \pm\sqrt{\frac{\kappa_1}{2} \pm \frac{1}{2}\sqrt{\kappa_1^2 - 4\kappa_2}} \qquad \text{(F7)}$$

From equation (F4),

$$A_1 = 0, \; A_3 = 0$$

Equation (F7) implies

$$\left.\begin{aligned} \beta_2 &= -\beta_1 \qquad \beta_4 = -\beta_3 \qquad \gamma_2 = -\gamma_1 \qquad \lambda_2 = -\lambda_1 \\ \delta_2 &= \delta_1 \qquad \delta_4 = \delta_3 \qquad \gamma_4 = -\gamma_3 \qquad \lambda_4 = -\lambda_3 \end{aligned}\right\} \qquad \text{(F8)}$$

Boundary conditions (F5) and (F6) lead to the following set of equations for the arbitrary constants:

$$\left.\begin{aligned}
&\sum_{\nu=1}^{4} B_\nu e^{\beta_\nu |x_1|} = A_0 \\
&\sum_{\nu=1}^{4} \gamma_\nu B_\nu e^{\beta_\nu |x_1|} = S_A x_1 \\
&\sum_{\nu=1}^{4} \delta_\nu B_\nu e^{\beta_\nu |x_1|} = A_2 \\
&\sum_{\nu=1}^{4} \lambda_\nu B_\nu e^{\beta_\nu |x_1|} = -\frac{2}{3} S_A x_1 \\
&\sum_{\nu=1}^{4} (4 + 5\delta_\nu - 8\gamma_\nu) B_\nu e^{\beta_\nu |x_2|} = 0 \\
&\sum_{\nu=1}^{4} (1 - 5\delta_\nu + 8\lambda_\nu) B_\nu e^{\beta_\nu |x_2|} = 0
\end{aligned}\right\} \quad \text{(F9)}$$

Equations (F9) were solved for A_0, A_2, B_1, B_2, B_3, and B_4 in terms of the other known quantities. In the process, $e^{\beta |x_1|}$ was approximated by $1 + \beta|x_1|$, since the latter is the asymptotic expression approached as $x_1 \to 0$. The limit was taken as $x_1 \to 0$ to give $2x_1 S_A = 1$. The constants A_0 and A_2 were eliminated, and B_1, B_2, B_3, and B_4 were finally solved in terms of b_0 and b_1 and then substituted back into (F2). The values are:

$$B_1 = -0.00376632 \qquad B_3 = -0.0694369$$

$$B_2 = 0.932918 \qquad B_4 = 1.399507$$

The total flux $F_0(x)$ was plotted against x (fig. 2), and the total number of absorptions and leakage from the slab were computed and compared with the values obtained by the numerical and Monte Carlo methods.

REFERENCES

1. Weinberg, Alvin M., and Noderer, L. C.: Theory of Neutron Chain Reactions, Vol. I. AECD-3471, AEC, May 15, 1951. (Contract W-7405-Enj-26.)

2. Kahn, Herman: Applications of Monte Carlo. RM 1237-AEC, The RAND Corp., Apr. 19, 1954. (Revised Apr. 27, 1956.)

3. Carlson, Bengt G.: Solution of the Transport Equation by S_n Approximations. LA-1599, Los Alamos Sci. Lab., Univ. Calif., Oct. 1953.

4. DeMarcus, Wendell C., and Nelson, Lewis: Methods of Probabilities in Chains Applied to Particle Transmission Through Matter. Appl. Math. Ser. 12, NBS, June 11, 1951.

5. Rockwell, Theodore, III, ed.: Reactor Shielding Design Manual. TID-7004, AEC, Mar. 1956.

6. Glasstone, Samuel, and Edlund, Milton C.: The Elements of Nuclear Reactor Theory. D. Van Nostrand Co., Inc., 1952.

TABLE I. - NUMERICAL-METHOD RESULTS FOR SLAB OF SKETCH (a)*

(a) Fluxes

[Flux to left of x_0 equals flux to right of x_0 taken as origin.]

Subregion to right of x_0	1	2	3	4	5	6	7	8	9	10
Numerical flux	2.464	1.720	1.406	1.188	1.016	0.873	0.749	0.637	0.533	0.430
Coordinate, x	.05	.15	.25	.35	.45	.55	.65	.75	.85	.95
Transport-theory flux (P_3) evaluated at x	2.073	1.754	1.489	1.268	1.082	.922	.783	.658	.546	.442

(b) Transmissions (per thousand source neutrons)

K	$P_K^T \times 10^3 = P_K^{-T} \times 10^3$	K	$P_K^T \times 10^3 = P_K^{-T} \times 10^3$
0	49.60	11	1.13
1	†47.03	12	.755
2	37.12	13	.503
3	26.91	14	.335
4	18.71	15	.223
5	12.74	16	.148
6	8.58	17	.099
7	5.74	18	.066
8	3.83	19	.044
9	2.56		
10	1.70		

*Numerical total leakage/sec = 0.43556 per source neutron; numerical total absorption/sec = 0.56402 per source neutron.

P_3 total absorption/sec = $2\Sigma_a \Delta X \sum_{i=1}^{10} \Phi(i) = 2 \times 0.2560 \times 0.1 \times 11.0161 = 0.56402$;

P_3 total leakage/sec = 1 - 0.56402 = 0.43598.

Sketch (a), worked as a two-region slab, yielded identical results; using 100 subregions instead of 20 yielded results virtually indistinguishable (small fraction of a percent) from those listed here.

†P_1^{LR} = 12.18/1000.

TABLE II. - MONTE CARLO RESULTS FOR SLAB OF SKETCH (a) FOR 10,700 HISTORIES*

(a) Fluxes

[Origin taken at x_0.]

Subregion	1	2	3	4	5	6	7	8	9	10
- Side of origin	2.438	1.686	1.414	1.201	0.9680	0.8850	0.7427	0.6070	0.5084	0.3968
+ Side of origin	2.521	1.796	1.419	1.242	1.072	.9065	.7457	.5941	.5299	.4212
Average	2.480	1.741	1.417	1.222	1.020	.8959	.7442	.6005	.5192	.4090

(b) Transmissions (per thousand source neutrons)

K	$P_K^T \times 10^3$	$P_K^{-T} \times 10^3$	Average, per thousand source neutrons
0	50.47	49.53	50.00
1	46.95	48.67	†47.81
2	35.05	35.47	35.26
3	26.85	24.74	25.70
4	19.52	18.37	18.95
5	12.65	13.32	12.99
6	9.58	8.43	9.00
7	5.74	5.27	5.50
8	3.83	4.28	4.06
9	2.41	2.99	2.70
10	1.72	1.93	1.82
11	1.12	.939	1.03
12	.770	.719	.745
13	.493	.478	.486
14	.374	.345	.360
15	.230	.217	.224
16	.186	.184	.185
17	.071	.105	.088
18	.071	.069	.070
19	.057	.046	.052

*Total leakage/sec = 0.43406/source neutron; total absorption/sec = 0.56569/source neutron (as computed from $2\sum_{i=1}^{10} \bar{\Phi}(i)\Sigma_a \Delta X$).

†P_1^{LR} = 11.97/1000.

TABLE III. - NUMERICAL RESULTS FOR TWO-REGION UNSYMMETRICAL SLAB

Transmissions			Flux		
K	$P_K^{-T} \times 10^4$	$P_K^{T} \times 10^4$	Subregion	Successive-collision solution	Simultaneous-equation solution
				Region I	
0	5000.00	88.607	1	2.1686	2.1686
1	989.99	96.626	2	1.5337	1.5337
2	401.50	93.172	3	1.3058	1.3059
3	200.73	81.131	4	1.1601	1.1601
4	112.27	66.091	5	1.0522	1.0522
5	67.200	51.467	6	.9663	.9663
6	42.061	38.847	7	.8947	.8947
7	27.149	28.684	8	.8334	.8334
8	17.910	20.851	9	.7797	.7797
9	12.002	14.989	10	.7319	.7319
10	8.135	10.689	11	.6889	.6889
11	5.559	7.578	12	.6498	.6498
12	3.822	5.351	13	.6140	.6140
13	2.639	3.767	14	.5811	.5811
14	1.828	2.646	15	.5506	.5506
15	1.269	1.856	16	.5223	.5223
16	.8826	1.300	17	.4959	.4959
17	.6146	.9100	18	.4712	.4712
18	.4283	.6366	19	.4481	.4481
19	.2986	.4451	20	.4263	.4263
20	.2083	.3111	21	.4058	.4058
21	.1454	.2175	22	.3865	.3865
22	.1015	.1520	23	.3683	.3683
23	.0709	.1062	24	.3511	.3511
24	.0495	.0742	25	.3348	.3348
25	.0346	.0518	26	.3193	.3193
26	.0241	.0362	27	.3047	.3047
27	.0162	.0253	28	.2909	.2909
28	.0118	.0177	29	.2778	.2778
			30	.2655	.2655
			31	.2539	.2539
			32	.2430	.2430
			33	.2330	.2330
			34	.2242	.2242
				Region II	
			35	0.2176	0.2176
			36	.2089	.2089
			37	.1992	.1992
			38	.1888	.1888
			39	.1780	.1781
			40	.1668	.1668
			41	.1551	.1551
			42	.1428	.1428
			43	.1297	.1297
			44	.1150	.1150

TABLE IV. - MONTE CARLO RESULTS FOR TWO-REGION UNSYMMETRICAL SLAB (25,000 HISTORIES)

Transmissions			Flux	
K	$P_K^{-T} \times 10^4$	$P_K^{T} \times 10^4$	Subregion	Results
			Region I	
0	5088.40	85.200	1	2.0935
1	976.320	96.160	2	1.4811
2	382.992	92.080	3	1.3003
3	190.118	78.928	4	1.1233
4	107.404	68.326	5	1.0222
5	69.601	46.642	6	.9665
6	44.012	38.743	7	.8733
7	29.416	27.141	8	.8096
8	17.702	20.134	9	.7981
9	12.614	14.028	10	.7671
10	8.228	10.232	11	.7166
11	5.784	8.857	12	.6441
12	4.009	5.018	13	.5930
13	2.429	3.975	14	.5452
14	1.617	2.293	15	.5542
15	1.014	1.947	16	.5142
16	.9172	.9563	17	.4909
17	.4454	.7925	18	.4383
18	.4675	.4472	19	.4172
19	.3435	.4270	20	.4530
20	.2552	.2319	21	.3996
21	.2036	.4757	22	.3864
22	.0593	.1833	23	.3354
23	.0683	.1395	24	.3418
24	.0599	.0955	25	.3189
25	.0427	.0310	26	.3245
26	.0304	.0399	27	.3212
27	.0104	.0448	28	.2792
28	.0055	.0116	29	.2876
			30	.2717
			31	.2591
			32	.2505
			33	.2366
			34	.2260
			Region II	
			35	0.1953
			36	.1947
			37	.1902
			38	.1893
			39	.1906
			40	.1581
			41	.1341
			42	.1333
			43	.1430
			44	.1049

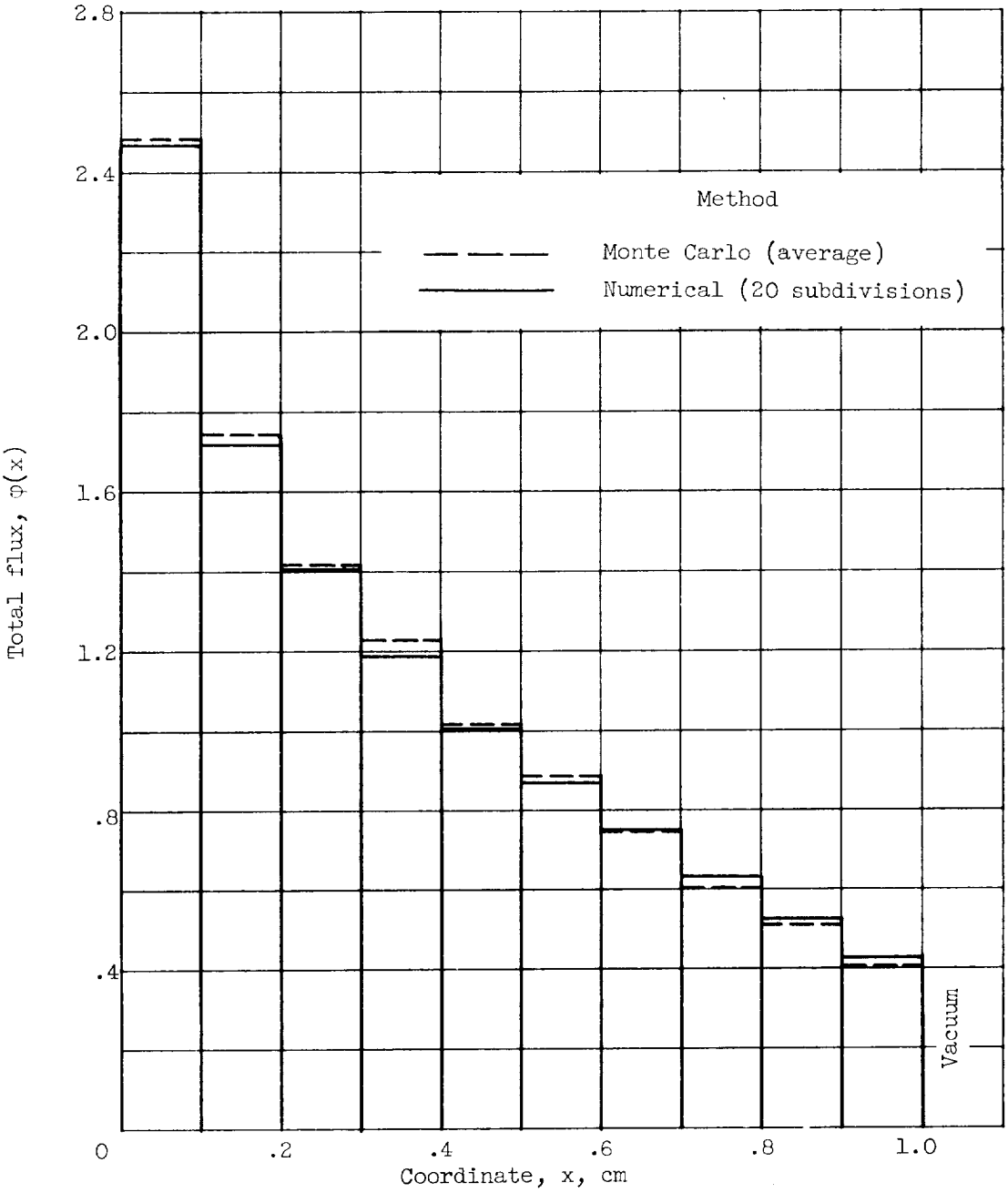

Figure 1. - Comparison of Monte Carlo and numerical-method solutions. Total mean free path, λ, 0.78125 centimeter per collision; scattering probability, λ/λ_s, 0.8.

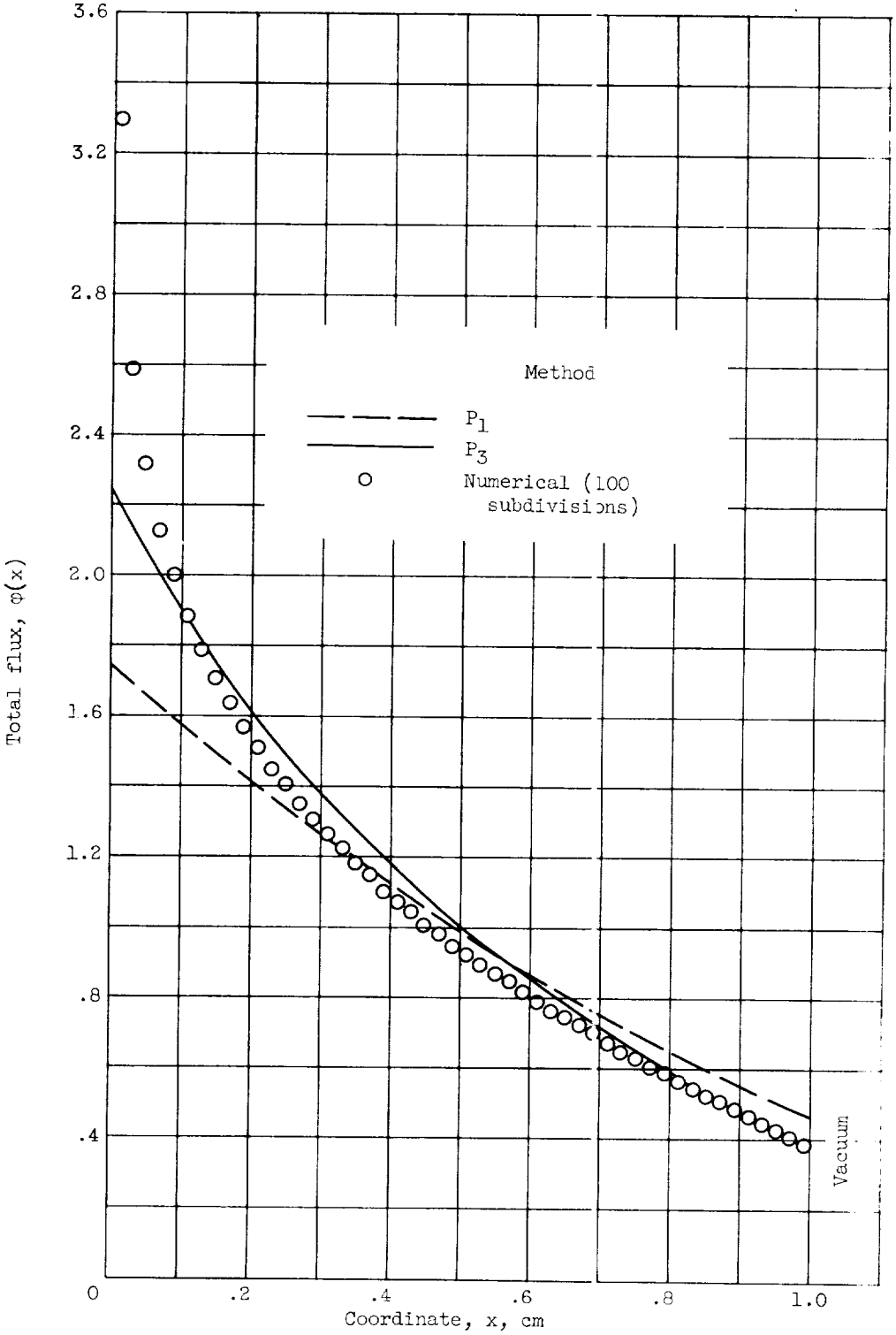

Figure 2. - Comparison of P_1, P_3, and 100-subregion-numerical-method solutions. Total mean free path, λ, 0.78125 centimeter per collision; scattering probability, λ/λ_s, 0.8.

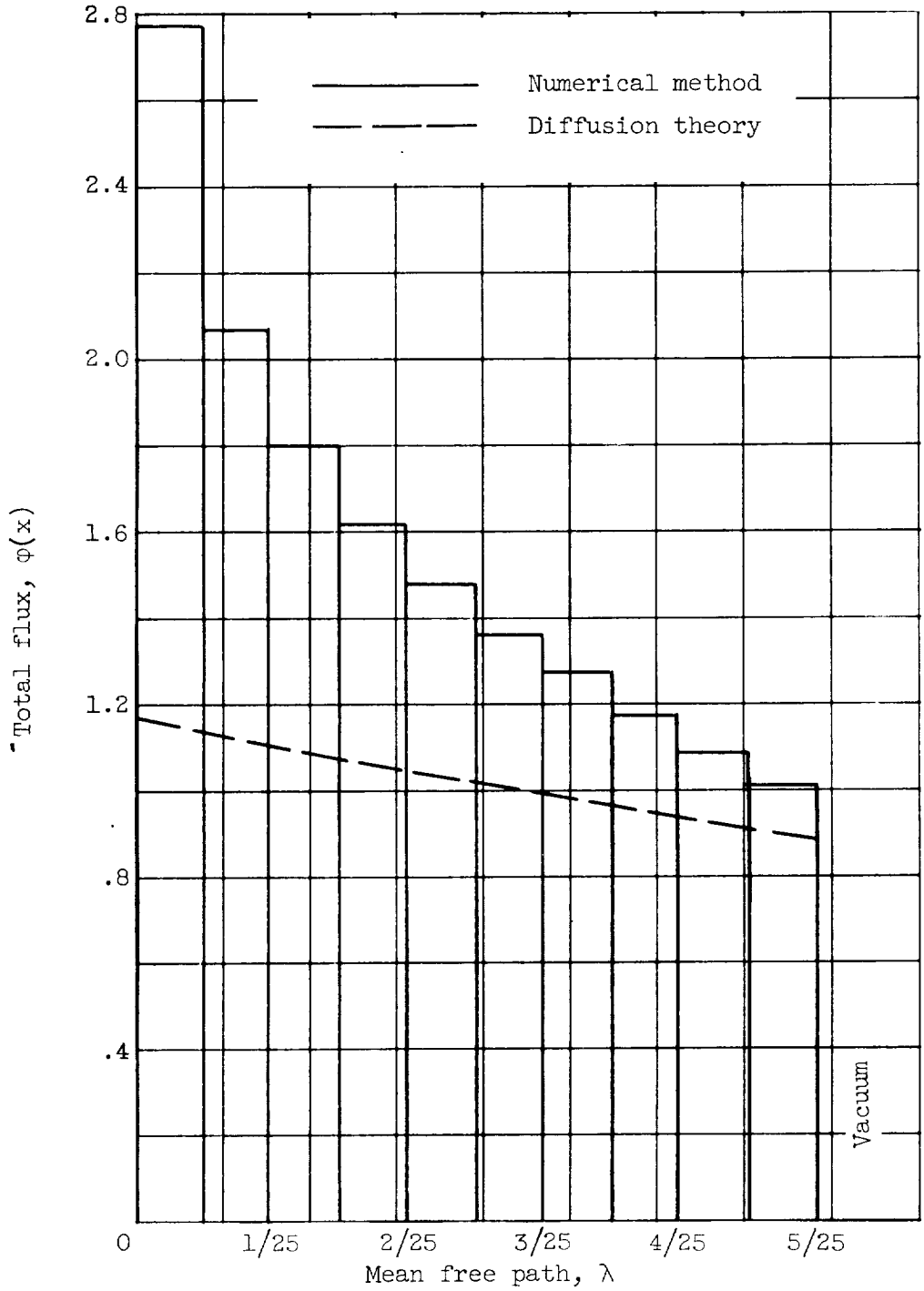

Figure 3. - Numerical and diffusion-theory curves for symmetrical slab of 1/5 mean free path half-thickness. Total mean free path, λ, 0.78125 centimeter per collision; scattering probability, λ/λ_s, 0.8.

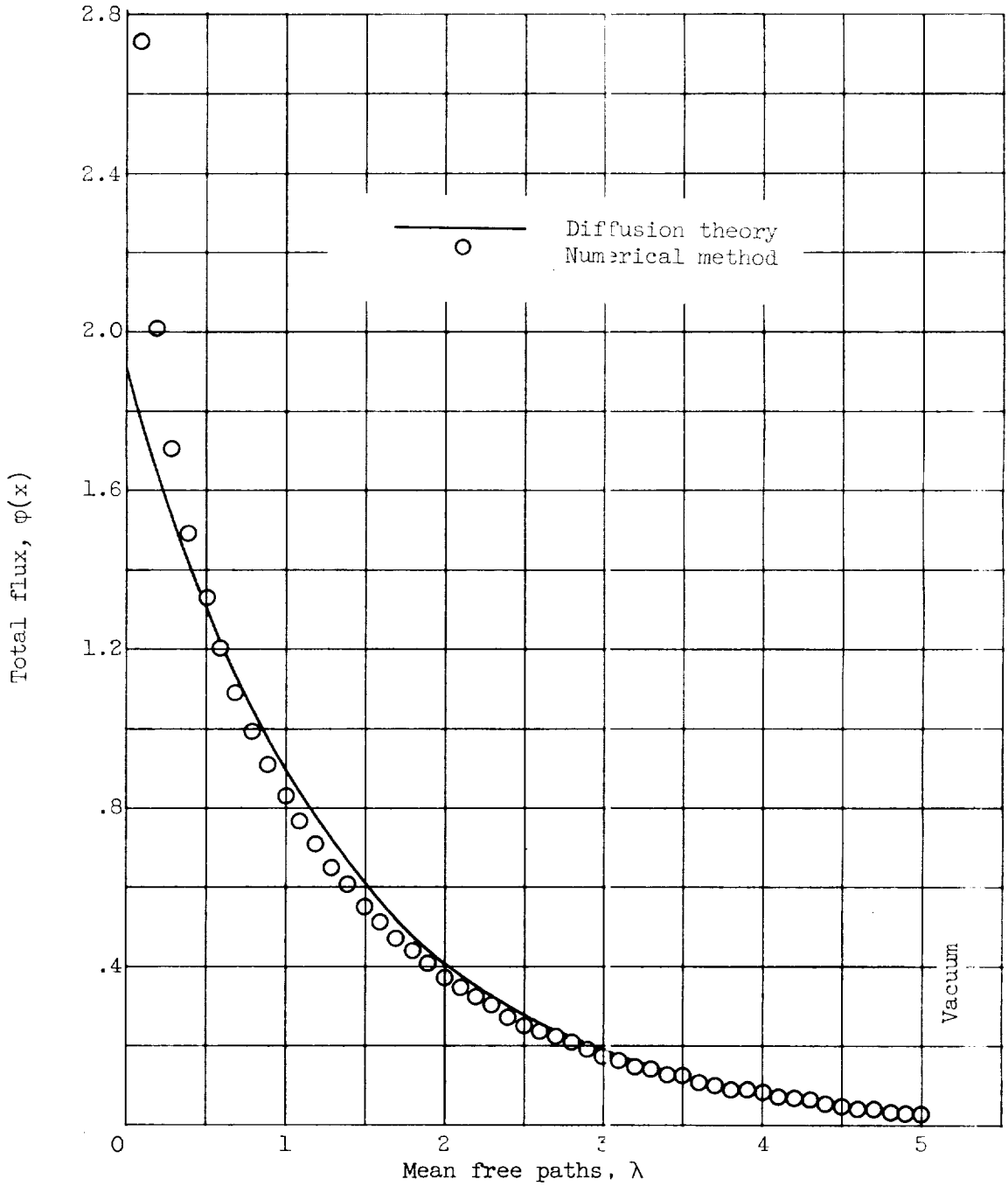

Figure 4. - Numerical and diffusion-theory curves for symmetrical slab of 5 mean free paths half-thickness. Total mean free path, λ, 0.78125 centimeter per collision; scattering probability, λ/λ_s, 0.8.

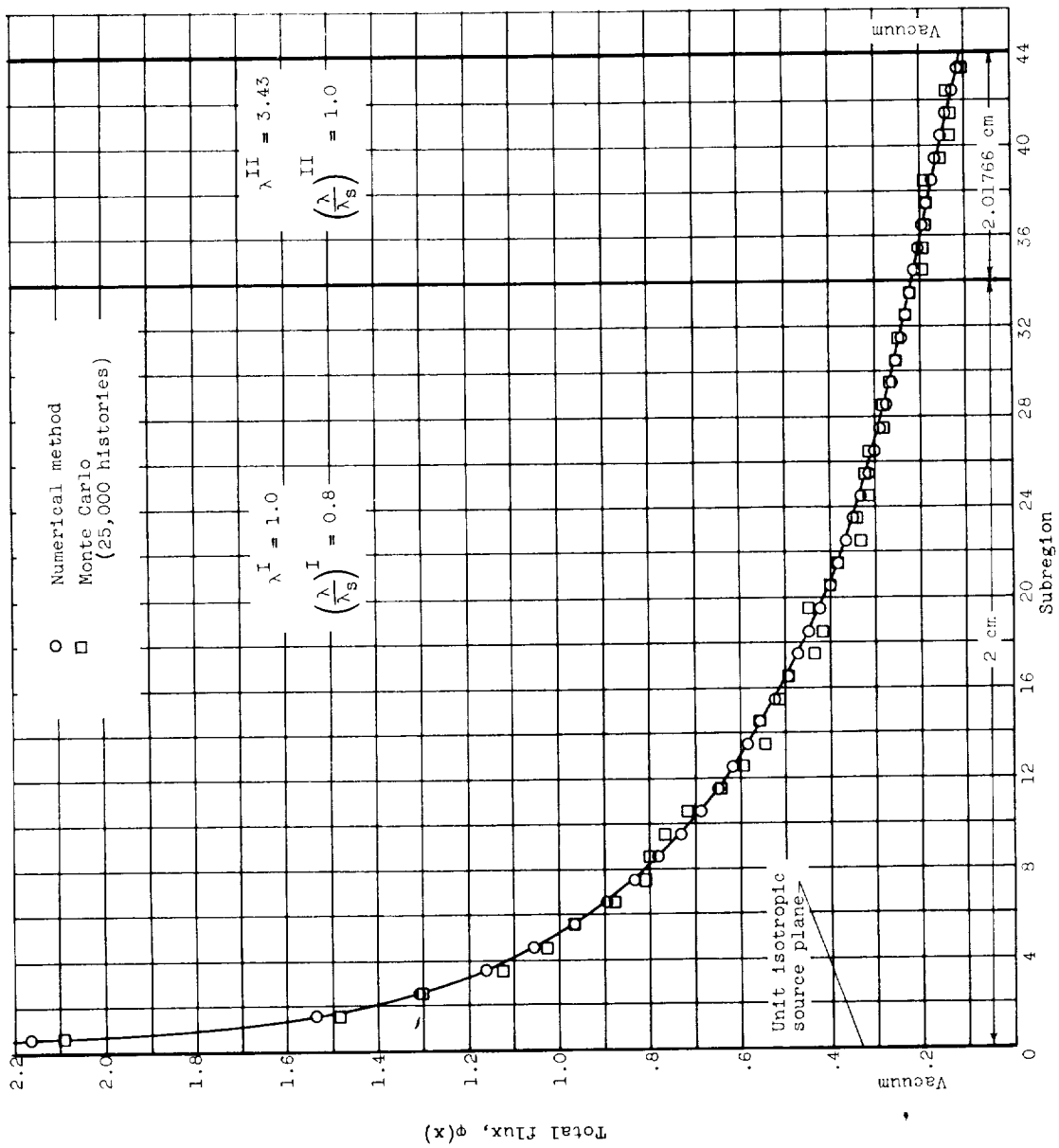

Figure 5. - Numerical-method flux and Monte Carlo flux for unsymmetrical double-slab problem.